Geometric Leaves of Symplectic Groupoids

Erik BRODSKY [a], *Leonid CHEKHOV* [b], *Pranjal DANGWAL* [c], *Skyler HAMLIN* [d], *Xu LIAN* [e], *Michael SHAPIRO* [b], *Samuel SOTTILE* [d] *and Jenny ZHAN* [f]

[a] *Department of Mathematics, Cornell University, 310 Malott Hall, Ithaca, NY 14853, USA*
E-mail: *eab384@cornell.edu*

[b] *Department of Mathematics, Michigan State University, East Lansing, MI 48823, USA*
E-mail: *chekhov@msu.edu*, *mshapiro@msu.edu*

[c] *360 Vincent Hall, 206 Church Street SE, Minneapolis, MN 55455, USA*
E-mail: *pdangwal@umn.edu*

[d] *Department of Mathematics, Stanford University, Building 380, Stanford, CA 94305, USA*
E-mail: *hamlin@stanford.edu*, *sottile@stanford.edu*

[e] *School of Mathematical Sciences, Nankai University, No 94. Weijin Road, Tianjin, 300071, P.R. China*
E-mail: *xulian189@outlook.com*

[f] *Department of Mathematics, University of Washington, Box 354350, C-138 Padelford, Seattle, WA 98195-4350, USA*
E-mail: *zzhan4@uw.edu*

Received March 05, 2025, in final form October 26, 2026; Published online November 11, 2026
https://doi.org/10.3842/SIGMA.2026.112

Abstract. A symplectic groupoid of triangular bilinear forms consists of pairs of matrices (B, A) with $A \in \mathcal{A}$—the set of real unipotent upper-triangular matrices—and $B \in \mathrm{SL}_n(\mathbb{R})$ such that $\widetilde{A} = BAB^{\mathsf{T}} \in \mathcal{A}$. The symplectic groupoid possesses a nondegenerate symplectic structure which induces a reflection-equation Poisson algebra on $\mathcal{A}$. Fock and Chekhov defined a Poisson map from the Teichmüller space $\mathcal{T}_{g,s}$ of genus g surfaces with s (one or two) holes to the space of unipotent upper-triangular $n \times n$ matrices; the image of this map forms a *geometric locus*. A matrix A in the geometric locus satisfies the *rank condition*: $\operatorname{rank}\left(A + A^{\mathsf{T}}\right) \leq 4$ and an additional positivity condition. We describe the coisotropic reduction of the Poisson cluster variety of $\mathcal{A}$ by the rank condition for $n = 5$ and 6 and show that these coisotropic reductions yield the corresponding geometric loci. Moreover, we analyze in both cases the cluster structures obtained by coisotropic reductions and recover the celebrated cluster structure of $\mathcal{T}_{2,1}$ for $n = 5$ and $\mathcal{T}_{2,2}$ for $n = 6$. We also discuss the positivity of the geometric cluster variables for $n = 3, 4, 5, 6$.

Key words: symplectic groupoid; Poisson structure; Goldman bracket; coisotropic reduction

2020 Mathematics Subject Classification: 53D30; 53D20; 81R12

1 Introduction

The study of the cluster structure of the *symplectic groupoid* of unipotent upper-triangular $n \times n$ matrices was initiated in [4, 5]. This paper continues this line of research by exploring the correspondence between the cluster realization of the Teichmüller space $\mathcal{T}_{g,s}$ of genus g surfaces with s holes, where $g \geq 1$, $s \in \{1, 2\}$ and the cluster structure of the *symplectic groupoid* of unipotent upper-triangular $n \times n$ matrices.

Let $\mathcal{A}_n$ denote the affine space of real unipotent upper-triangular $n \times n$ matrices. The symplectic groupoid $\mathfrak{M}_n$ of the unipotent upper-triangular $n \times n$ matrices is the set of pairs

$$\mathfrak{M}_n = \{(B, A) \mid B \in \mathrm{SL}_n,\ A \in \mathcal{A}_n \text{ such that } BAB^{\mathsf{T}} \in \mathcal{A}_n\}.$$

The space $\mathfrak{M}_n$ possesses a natural symplectic structure [18]. The pushforward of the dual Poisson bracket under the projection $(B, A) \mapsto A$ induces the Poisson bracket on $\mathcal{A}_n$ studied in [1, 2] and called the *Bondal Poisson bracket*.

The Teichmüller space $\mathcal{T}_{g,s}$ of genus g Riemann surfaces with s holes is a Poisson variety equipped with the renowned Goldman Poisson bracket. Define

$$\mathrm{par}(n) = \begin{cases} 1, & \text{if } n \text{ is odd,} \\ 2, & \text{otherwise.} \end{cases}$$

In [3], a Poisson map $\varphi\colon \mathcal{T}_{\lfloor (n-1)/2 \rfloor, \mathrm{par}(n)} \to \mathcal{A}_n$ was constructed. The map $\varphi\colon \mathcal{T}_{\lfloor (n-1)/2 \rfloor, \mathrm{par}(n)} \to \mathrm{Im}(\varphi)$ is a finite covering map. Notice that $\dim(\mathcal{T}_{\lfloor (n-1)/2 \rfloor, \mathrm{par}(n)}) = 3n - 6$ and $\dim(\mathcal{A}_n) = \binom{n}{2}$. The dimensions of the corresponding generic symplectic leaves are $3n-6-\mathrm{par}(n)$ and $\binom{n}{2} - \lfloor \frac{n}{2} \rfloor$. For $n = 3$ the dimensions of symplectic leaves coincide and both equal 2; for $n = 4$ the dimensions are 4, and for $n = 5$ they are 8. However, in the latter case, the dimensions of the spaces are different, $\dim(\mathcal{T}_{2,1}) = 9$ with one central element while $\dim(\mathcal{A}_5) = 10$ with two central elements.

We call the image $\mathrm{Im}(\varphi)$ *a geometric locus* of $\mathcal{A}_n$. It is the union of symplectic leaves in $\mathcal{A}_n$ called *geometric leaves*. For $n \geq 6$, the dimension of a geometric leaf is smaller than the dimension of a generic symplectic leaf in $\mathcal{A}_n$. In [4], Chekhov and Shapiro constructed a Poisson cluster algebra $\mathcal{X}(\mathcal{A}_n)$ together with a finite Poisson map $\xi\colon \mathbb{C}[\mathcal{A}_n] \to \mathcal{X}(\mathcal{A}_n)$, where $\mathbb{C}[\mathcal{A}_n]$ is the Poisson algebra of regular functions on $\mathcal{A}_n$ equipped with the Bondal Poisson bracket and $\mathcal{X}(\mathcal{A}_n)$ is equipped with the cluster Poisson structure. We note that $\mathrm{Im}(\varphi)$ satisfies the so-called *rank condition*. We use the rank condition to describe a coisotropic reduction of $\mathcal{X}(\mathcal{A}_n)$ for $n = 5$ and 6. We prove that the Poisson algebra obtained as the result of the reduction for $n = 5, 6$ inherits a cluster structure from $\mathcal{X}(\mathcal{A}_n)$ and coincides with the corresponding renowned cluster algebras $\mathcal{X}\big(\mathcal{T}_{\lfloor (n-1)/2 \rfloor, \mathrm{par}(n)}\big)$ whose seeds are labeled by ideal triangulations of hyperbolic surfaces of genus $\lfloor \frac{n-1}{2} \rfloor$ with $\mathrm{par}(n)$ holes (see Section 3).

Note that, besides the rank condition, genuine geometric leaves must also satisfy the *positivity condition*, which requires that all geometric cluster variables obtained from cluster variables of $\mathcal{A}_n$ quivers by reduction maps be positive. We call the subset of $\mathcal{A}_n$ that satisfies the rank condition the *pre-geometric locus*. It is foliated by symplectic leaves called *pre-geometric leaves*. Although a complete analysis of the positivity condition for all possible schemes of coisotropic reduction is beyond the scope of this paper, in two appendices we classify all genuine geometric leaves obtained in the simplest cases of coisotropic reductions for $n = 5$ and 6. We show that these geometric leaves are preserved by the braid-group action of the $\mathcal{A}_n$ quiver, thus proving the consistency of the geometric reduction procedure.

In Section 2, we review the definitions of Poisson varieties and cluster structures compatible with Poisson brackets. In Section 3, we recall the definition of the shear coordinates on the Teichmüller space $\mathcal{T}_{g,s}$. In Section 4, we recall the construction of the symplectic groupoid of the unipotent upper-triangular matrices and the corresponding Poisson bracket on $\mathcal{A}_n$, while, in Section 5, we describe the construction of log-canonical parameters for the symplectic groupoid [4].

In Section 6, we compare the dimensions of a pre-geometric leaf and $\mathcal{A}_n$ for $n \geq 3$. In Section 7, we state the necessary condition for a pre-geometric leaf (called *the rank condition*).

Definition 1.1. For an $n \times n$ unipotent upper-triangular matrix A, we call the condition $\mathrm{rank}\big(A + A^{\mathsf{T}}\big) \leq 4$ *the rank condition*.

Finally, in Section 8 we provide solutions of the rank condition for $n = 3, 4, 5$ and 6.

2 Cluster algebras and Poisson geometry

2.1 Preliminaries

We start by recalling the definition of a cluster algebra and a compatible Poisson structure.

Definition 2.1. A *quiver* is a directed graph which we shall represent by the tuple $Q = (V, E, s, t)$. V and E are the *vertex* and *edge sets*, respectively, and $s, t\colon E \to V$ are the *source* and *target maps*.

We will call the elements of the directed edge set E *arrows*. Moreover, for an arrow $\alpha \in E$, $s(\alpha) \in V$ is called the *source* or *starting* vertex and $t(\alpha) \in V$ the *target* or *terminal* vertex. In keeping with cluster algebra convention, we shall require our quivers to have no oriented 1-cycles (loops) or oriented 2-cycles. We consider only finite quivers with $|V| < \infty$ and $|E| < \infty$.

Definition 2.2. Let Q be a quiver whose set of vertices V is partitioned into two disjoint subsets V_m of *mutable* vertices and V_f of *frozen* vertices. To each vertex $k \in V_m$, one can associate a *quiver mutation* μ_k. This mutation μ_k at vertex k transforms Q into a new quiver $Q' = \mu_k(Q)$ via a sequence of three steps:

(1) for each oriented two-arrow path $i \to k \to j$, introduce a new arrow $i \to j$;

(2) reverse the direction of all arrows incident to the vertex k;

(3) consecutively remove all oriented 2-cycles created in step (1).

It is an easy exercise to show that for any quiver Q and any vertex k in Q, μ_k is an involution on Q.

Definition 2.3. Let Q be a quiver and let V denote its vertex set. A *seed* associated with Q is a tuple $i = (Q, \{X_k\}_{k\in V})$, where $\{X_k\}_{k\in V}$ is a set of independent variables generating the ambient field $\mathcal{F}$ of rational functions of $X_1, X_2, \ldots$.

We now present an equivalent definition of *quiver mutation* in terms of *skew-symmetric* matrices. We restrict our attention here to *skew-symmetric coefficient-free* cluster algebras.

Remark 2.4. For a more general treatment of the subject, the reader is referred to [9, 12]. In the current paper, a more general definition of a *skew-symmetrizable cluster algebra with geometric coefficients* is not used.

Definition 2.5. Let $B = (b_{ij})$ be a skew-symmetric $n \times n$ integer matrix. For $k \in [1, n]$, the *matrix mutation* μ_k in direction k transforms B into the $n \times n$ matrix $\mu_k(B) = B' = (b'_{ij})$ with the entries defined as

$$b'_{ij} = \begin{cases} -b_{ij} & \text{if } i = k \text{ or } j = k, \\ b_{ij} + \dfrac{|b_{ik}|b_{kj} + b_{ik}|b_{kj}|}{2} & \text{otherwise.} \end{cases} \tag{2.1}$$

Remark 2.6. The information in any directed graph can be recorded in a skew-symmetric integer matrix B by defining b_{ij} to be the number of arrows from vertex i to j minus the number of arrows from j to i. This matrix is called the *signed incidence matrix* of the graph. Observe that since we do not allow loops in a quiver, the diagonal entries of the incidence matrix of a quiver are always 0. Thus, quivers give rise to skew-symmetric matrices, and it is easy to verify that the above Definition 2.5 of matrix mutations agrees with Definition 2.2 of quiver mutations given earlier in this section.

Definition 2.7. A *seed* in $\mathcal{F}$ is a pair $(\mathbf{x}, B)$, where B is a skew-symmetric $n \times n$ integer matrix and $\mathbf{x} = (x_1, \dots, x_n)$ is a collection of *cluster* variables forming a transcendence basis of $\mathcal{F}$. The tuple $\mathbf{x}$ is called a *cluster*, and n is the *rank* of the cluster algebra.

Definition 2.8. Given a seed $(\mathbf{x}, B)$ as above, the *seed mutation* μ_k ($k \in [1, n]$) transforms $(\mathbf{x}, B)$ into a new seed $\mu_k(\mathbf{x}, B) = (\mathbf{x}', B')$ such that

- $B' = \mu_k(B)$ (see formula (2.1)),
- $x'_j = (\mathbf{x}')_j$ satisfies the so-called *x-variable mutation rule*:

$$x'_i = \mu_k(x_i) = \begin{cases} x_i^{-1} & \text{if } i = k, \\ x_i\big(1 + x_k^{-\operatorname{sgn}(b_{ik})}\big)^{-b_{ik}} & \text{if } i \neq k, \end{cases}$$

where

$$\operatorname{sgn}(z) := \begin{cases} 1 & \text{if } z > 0, \\ 0 & \text{if } z = 0, \\ -1 & \text{if } z < 0. \end{cases}$$

Let x_1 be the set of cluster variables in a seed t. For the mutation μ_k, the allowed values of x_k are those satisfying $x_k \neq -1$. Note that the condition $x_k \neq -1$ is equivalent to the condition $\mu_k(x_k) \neq -1$ in the seed $\mu_k(t)$.

2.2 Compatible Poisson brackets

In this subsection, we recall some basic definitions of Poisson geometry and the notion of a Poisson structure compatible with the cluster algebra structure first introduced in [10].

A *Poisson algebra* is a commutative associative algebra $\mathcal{A}$ equipped with a *Poisson bracket* $\{\cdot,\cdot\}\colon \mathcal{A} \times \mathcal{A} \to \mathcal{A}$ that is a skew-symmetric bilinear map satisfying

(1) the *Leibniz identity* $\{fg, h\} = f\{g, h\} + \{f, h\}g$, and

(2) the *Jacobi identity* $\{f, \{g, h\}\} + \{g, \{h, f\}\} + \{h, \{f, g\}\} = 0$

for functions f, g, h.

A *Casimir element of* $\mathcal{A}$ is an element $c \in \mathcal{A}$ such that $\{c, f\} = 0$ for any $f \in \mathcal{A}$. By an abuse of notation, we also call Casimir elements *Casimir functions* or, simply, *Casimirs*. A smooth real manifold M is said to be a *Poisson manifold* if the algebra $C^\infty(M)$ of smooth functions on M is a Poisson algebra. In this case, we say that M is equipped with a *Poisson structure*.

Let $\{\cdot,\cdot\}$ be a Poisson bracket on the ambient field $\mathcal{F}$ considered as the field of rational functions in n independent variables with rational coefficients. We say that the collection of functions $\mathbf{f} = (f_1, \dots, f_n)$ is *log-canonical* with respect to the bracket $\{\cdot,\cdot\}$ if $\{f_i, f_j\} = \omega_{ij} f_i f_j$, where ω_{ij} are constants for all $i, j \in [1, n]$. The *coefficient matrix* of $\{\cdot,\cdot\}$ is defined to be $\Omega^{\mathbf{f}} = (\omega_{ij})_{i,j=1}^n$. Due to the antisymmetry of $\{\cdot,\cdot\}$, the coefficient matrix is evidently skew-symmetric.

Definition 2.9. A cluster structure is *compatible* with a Poisson bracket if any cluster is log-canonical with respect to the bracket.

Remark 2.10. It is well known that any cluster structure has a compatible Poisson structure [12] that, in the cluster $\mathbf{x} = (x_1, \dots, x_n)$, takes the form $\{x_i, x_j\} = B_{ij} x_i x_j$. Recall that B is an integer skew-symmetric matrix.

One of the well-known examples of a cluster algebra equipped with a natural Poisson bracket is provided by the Teichmüller space equipped with the Goldman Poisson bracket [7, 8, 11].

3 Description of cluster coordinates of the Teichmüller space $\mathcal{T}_{g,s}$, $s \geq 1$

The topology of an oriented, complete, two-dimensional surface is determined by its genus g and the number of boundary components, s. Such a surface will be denoted $\Sigma_{g,s}$. We assume that g, s satisfy the *hyperbolicity condition* $2g-2+s>0$.

The topological surface $\Sigma_{g,s}$ with g, s satisfying the hyperbolicity condition can be equipped with a hyperbolic metric, i.e., a metric with constant curvature -1; the surface with a hyperbolic metric is called a *hyperbolic surface*. Any hyperbolic surface is obtained as a quotient of the upper half plane $\mathbb{H}=\{x+\mathrm{i}y\in\mathbb{C}\mid x,y\in\mathbb{R},\, y>0\}$ by a discrete subgroup F of $\mathrm{PSL}(2,\mathbb{R})$ called a Fuchsian group. Note that $\mathbb{H}$ is equipped with the standard hyperbolic metric

$$\mathrm{d}s^2=\frac{\mathrm{d}x^2+\mathrm{d}y^2}{y^2}.$$

An element $g\in\mathrm{PSL}(2,\mathbb{R})$ represented by a 2×2 real matrix $g=\pm\left(\begin{smallmatrix}a & b\\ c & d\end{smallmatrix}\right)$ acts naturally on $\mathbb{H}$ via Möbius transformations, $z\mapsto\frac{az+b}{cz+d}$. This action is by isometries. On $\mathbb{H}$, the geodesics are given by semicircles centered on the real line and vertical lines. An ideal triangle in $\mathbb{H}$ is a triangle in the open upper half plane $\{(x,y)\mid y>0\}$ with geodesic sides and all three vertices on the real line, or two on the real line and one at infinity. All ideal triangles in $\mathbb{H}$ are isometric to each other. An *ideal triangle* of a hyperbolic surface is a triangle with geodesic sides isometric to one (and, hence, any) ideal triangle in $\mathbb{H}$.

For $2g-2+s>0$, each hyperbolic surface of genus g with s holes can be represented as a disjoint union of s topologically closed "outer" infinite hyperbolic domains ("holes"), each of which is isometric to a half of a one-sheeted hyperboloid whose geodesic boundary is a unique closed geodesic homeomorphic to a loop around a hole (a hole "boundary", or perimeter), and the remaining (topologically open but bounded) part, which we call the *reduced surface*. In what follows, a *hyperbolic surface* will always refer to this reduced surface. (The simplest reduced surface, $\Sigma_{0,3}$, is depicted in Figure 1.)

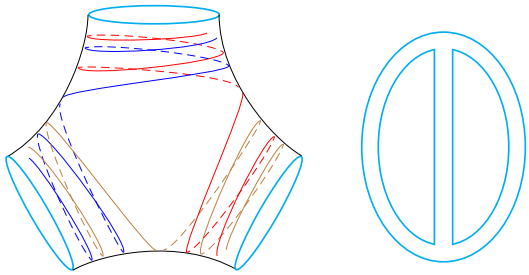


Figure 1. Splitting $\Sigma_{0,3}$ into two ideal triangles; three lines of the partition, or sides of the triangles, are indicated by three different colors. Each line has an infinite geodesic length, and each of its ends winds indefinitely toward the perimeter of a hole. The corresponding fat graph has three edges dual to the partition lines.

A fundamental domain is a subset of $\mathbb{H}$ that is a connected union of $4(g-1)+2s$ ideal triangles, which, upon the action of F on $\mathbb{H}$, transforms into an infinite ideal-triangle tessellation $\mathbb{T}$ of $\mathbb{H}-\{\bigcup^{\infty}C_{P_i}\}$, where C_{P_i} are disjoint closed semicircular domains bounded by all copies of boundary geodesics. Then $\Sigma_{g,s}=\big(\mathbb{H}-\{\bigcup^{\infty}C_{P_i}\}\big)\backslash F$, and we call an (ideal) triangulation T of $\Sigma_{g,s}$ the corresponding factor of the tessellation, $T=\mathbb{T}\backslash F$.

Therefore, an *ideal triangulation* of a hyperbolic surface is a partition of the reduced surface by geodesics that satisfies the following conditions:

- The surface is divided into regions, each of which is the interior of an ideal triangle.
- Each geodesic in the partition forms an edge of an embedded ideal triangle.
- The vertices of the ideal triangles are located at ideal points, which are points at infinity in hyperbolic geometry (the absolute).

In an ideal triangulation of a hyperbolic surface, each edge is a common side of two triangles that together form an ideal quadrilateral. A parameter, *the* (*exponential*) *shear coordinate*, can be assigned to each edge of an ideal triangulation by lifting to $\mathbb{H}$. The exponential shear coordinate is the cross-ratio of the four vertices of the lift of the ideal quadrilateral and is always a positive real number.

An ideal triangulation T of $\Sigma_{g,s}$ is dual to the *ribbon* (or *fat*) graph Γ whose vertices correspond to ideal triangles of T and edges of Γ are dual to the edges of T, that is, each edge of Γ intersects transversely exactly one edge of T at exactly one point. The ribbon graph is homotopy equivalent to the surface, in particular, $\pi_1(\Sigma_{g,s}, p) \simeq \pi_1(\Gamma, p)$ for any point $p \in \Gamma$. Any nontrivial element $\gamma \in \pi_1(\Sigma_{g,s}, p)$ has a unique representative as a closed path (sequence of edges of Γ with the same starting and end point) without backtracking. At the vertices of the ribbon graph, the incident half-edges have a cyclic order that is compatible with the orientation of the surface.

Example 3.1. The simplest example is $\Sigma_{0,3}$—the sphere with three holes also known as a pair of pants. The corresponding partition into ideal triangles and the fat graph dual to this partition are depicted in Figure 1.

On a hyperbolic surface Σ, a closed geodesic γ starting and ending at $p \in \Sigma$ can be lifted to a path $\tilde{\gamma}$ in the universal cover $\mathbb{H}$. The deck transformation of $\mathbb{H}$ given by $[\gamma] \in \pi_1(\Sigma)$ is represented by an element $M_\gamma \in \mathrm{PSL}(2,\mathbb{R})$ of the Fuchsian group of the surface. Following [6], we describe M_γ as a product of matrices:

$$L = \begin{bmatrix} 0 & 1 \\ -1 & -1 \end{bmatrix}, \qquad R = \begin{bmatrix} 1 & 1 \\ -1 & 0 \end{bmatrix}, \qquad X(x_t) = \begin{bmatrix} 0 & -\dfrac{1}{\sqrt{x_t}} \\ \sqrt{x_t} & 0 \end{bmatrix},$$

$$L_s := LX(s) = \begin{pmatrix} s^{-1/2} & 0 \\ -s^{-1/2} & s^{1/2} \end{pmatrix}, \qquad R_s := RX(s) = \begin{pmatrix} s^{-1/2} & -s^{1/2} \\ 0 & s^{1/2} \end{pmatrix},$$

where t is an edge of a ribbon graph describing the hyperbolic surface and $x_t > 0$ is the (exponential) shear parameter assigned to t. The path γ travels along the edges of the ribbon graph, turning right and left, which leads to the following product formula for the deck transformation M_γ with the composition law from right to left. Then, the *geodesic function* $G_\gamma := |\mathrm{tr} M_\gamma|$ is given by the well-known formula $G_\gamma = 2\cosh\left(\frac{l_\gamma}{2}\right)$ [3] in terms of the geodesic length l_γ.

Definition 3.2. The Teichmüller space $\mathcal{T}_{g,s}$ is the space of all hyperbolic surfaces of genus g with s holes (or, equivalently, complex structures on a genus g surface with s holes with a choice of basis of $H_1(\Sigma_{g,s}, \mathbb{Z})$).

4 Description of the space of objects $\mathcal{A}_n$ of the symplectic groupoid $\mathfrak{M}_n$

Definition 4.1 (see [2])**.** Bondal's *symplectic groupoid* $\mathfrak{M}_n$ *of unipotent upper triangular matrices* (or, *symplectic groupoid*, for brevity) is the groupoid with object set $\mathcal{A}_n$, the set of $n \times n$ unipotent real upper triangular matrices, and the set of morphisms from $A \in \mathcal{A}_n$ to $\widetilde{A} \in \mathcal{A}_n$, i.e., the set of matrices $B \in \mathrm{SL}(n,\mathbb{R})$ such that $\widetilde{A} = BAB^{\mathsf{T}}$.

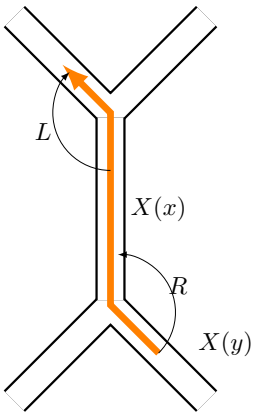


Figure 2. Factorization of the deck transformation operator. The deck transformation along path γ is expressed as a product of the matrix sequence $M_\gamma = \cdots L \cdot X(x) \cdot R \cdot X(y) \cdots = \cdots L_x \cdot R_y \cdots$.

For a more general notion of symplectic groupoid, see [18]. Note that $\mathfrak{M}_n$ is a submanifold of $\mathrm{SL}(n,\mathbb{R}) \times \mathcal{A}_n$ given by $\mathfrak{M}_n = \big\{(B,A) \mid B \in \mathrm{SL}(n,\mathbb{R}),\ A \in \mathcal{A}_n,\ BAB^{\mathsf{T}} \in \mathcal{A}_n\big\}$.

The *set of compatible pairs* is the fiber product $\mathfrak{M}_n \times_{\mathcal{A}_n} \mathfrak{M}_n$:

$$\mathfrak{M}_n^{(2)} = \big\{\big((C,\widetilde{A}),(B,A)\big) \mid C,B \in \mathrm{SL}(n,\mathbb{R}),\ A,\widetilde{A} \in \mathcal{A}_n, \\ \widetilde{A} = BAB^{\mathsf{T}},\ C\widetilde{A}C^{\mathsf{T}} \in \mathcal{A}_n\big\} \subset \mathfrak{M}_n \times \mathfrak{M}_n.$$

There are two natural projections $p_1, p_2 \colon \mathfrak{M}_n^{(2)} \to \mathfrak{M}_n$, projecting on the first and second coordinates respectively, in addition to a multiplication map $m \colon \big((C,BAB^{\mathsf{T}}),(B,A)\big) \mapsto (CB,A)$. There is a natural symplectic form ω on $\mathfrak{M}_n$ such that $m^*\omega = p_1^*\omega + p_2^*\omega$ [2]. The symplectic form ω defines a dual Poisson bracket on $\mathfrak{M}_n$. The pushforward of this Poisson bracket under the natural projection $\mathfrak{M}_n \to \mathcal{A}_n$ induces a Poisson bracket $\mathcal{P}_{\mathrm{sym}}$ on $\mathcal{A}_n$, studied in [2].

In particular, for any matrix $A \in \mathcal{A}_n$, consider the polynomial $\chi_A(\lambda) := \det\big(A + \lambda A^{\mathsf{T}}\big)$. Its coefficients are polynomial functions of the entries A_{ij} of A. They generate the algebra of Casimir functions with respect to the Poisson bracket on $\mathcal{A}_n$. It is easy to see that $\chi_A(\lambda) = \chi_{\widetilde{A}}(\lambda)$.

Remark 4.2. Note that the polynomial $\chi_A(\lambda)$ is reciprocal for any A and, hence, the coefficients contain only $\lfloor \frac{n}{2} \rfloor$ algebraically independent functions of A_{ij}.

5 Log-canonical coordinates for $\mathcal{A}_n$

In this section we recall the construction from [4] of log-canonical coordinates compatible with the Poisson bracket on $\mathcal{A}_n$. The Fock–Goncharov parameters Z_{ijk} for $n \times n$ upper-triangular matrices are log-canonical coordinates for the standard trigonometric Poisson-Lie bracket on SL_n. Parameters Z_{ijk} are organized in the triangular lattice. The corresponding log-canonical Poisson bracket $\mathcal{P}_{\mathrm{tr}}$ is described by the quiver on Figure 3. As explained in [4], Z_{ijk} parametrize, in particular, the Borel subgroup B_n of the upper triangular matrices which is a Poisson subgroup of SL_n and the log-canonical Poisson structure $\mathcal{P}_{\mathrm{tr}}$ coincides with the Poisson-Lie structure on B_n.

As the next step in [4], we use Z_{ijk} to construct log-canonical coordinates for the Poisson bracket on $\mathcal{A}_n$. Parameters Z_{ijk} describe three (non-independent) triangular matrices $\mathcal{M}_1$, $\mathcal{M}_2$, $\mathcal{M}_3$. Matrices $\mathcal{M}_i$ are boundary measurement matrices in the sense of A. Postnikov [16]. Below, we explain the construction in the case $n = 6$. We draw the following oriented graph Υ (see the black directed graph in Figure 4) dual to the original quiver (in blue). Let $\mathfrak{B}$ denote the set of triples of barycentric indices $\mathfrak{B} = \{(i_1,i_2,i_3) \mid 0 \le i_1,i_2\,i_3 \le 6 \text{ and } i_1+i_2+i_3 = 6\}$. For each oriented path p in Υ starting from one of the vertices $\{1,2,3,4,5,6\}$ on the right side of the

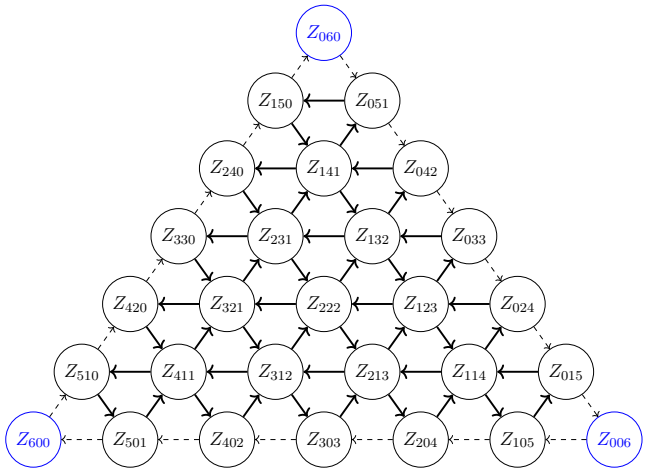


Figure 3. The Fock–Goncharov parameters organized in the triangular lattice. The quiver with vertices labeled by the Fock–Goncharov parameters $Z_{\alpha,\beta,\gamma}$ encodes the Poisson bracket between Z's: $\{Z_{\alpha,\beta,\gamma}, Z_{\alpha',\beta',\gamma'}\} = \varkappa \cdot Z_{\alpha,\beta,\gamma} \cdot Z_{\alpha',\beta',\gamma'}$. Here $\varkappa$ denotes the signed weight of the arrow between (α,β,γ) and (α',β',γ'). The coefficient $\varkappa = 1$ if there is a solid arrow from (α,β,γ) to (α',β',γ'), $\varkappa = -1$ if there is a solid arrow in the opposite direction; $\varkappa = \frac{1}{2}$ if the arrow from (α,β,γ) to (α',β',γ') is dashed, $\varkappa = -\frac{1}{2}$ if the arrow in the opposite direction is dashed; and $\varkappa = 0$ if (α,β,γ) and (α',β',γ') are disconnected.

triangle and terminating at one of the vertices $\{1',2',3',4',5',6'\}$ on the left side of the triangle, we denote by $\mathfrak{B}_p$ the subset of $\mathfrak{B}$ corresponding to vertices situated above the path p and we assign to the path its weight $w(p) = \prod_{\alpha\in\mathfrak{B}_p} Z_\alpha$.

Let $\mathfrak{P}_{ij}$ be the set of all oriented paths from j to i'. We define the entry $(\mathcal{M}_1)_{ij}$ of the matrix $\mathcal{M}_1$ to be $(\mathcal{M}_1)_{ij} = \sum_{p\in\mathfrak{P}_{ij}} w(p)$. Clearly, $\mathcal{M}_1$ is lower-triangular because there is no path in Υ from j to i' for $i < j$. To construct $\mathcal{M}_2$ we consider oriented paths in Υ from the right side $\{1,2,3,4,5,6\}$ to the bottom $\{1'',2'',3'',4'',5'',6''\}$. Denote the set of such paths connecting j to i'' by $\mathfrak{P}^1_{ij}$. Any such path p divides the triangle into two parts: the left part $\mathfrak{B}^l_p$ containing Z_{006} and Z_{600} and the right part $\mathfrak{B}^r_p$ containing Z_{060}. We recall that Fock–Goncharov parameters are obtained by restriction $Z_{00n} = Z_{0n0} = Z_{n00} = 1$ and set the weight $w(p) = \prod_{\alpha\in\mathfrak{B}^l_p} Z_\alpha$, and $(\mathcal{M}_2)_{ij} = \sum_{p\in\mathfrak{P}^1_{ij}} w(p)$. $\mathcal{M}_2$ is upper-triangular.

Finally, to construct $\mathcal{M}_3$, we obtain a new graph Υ' from Υ by rotating the graph Υ shown in black in Figure 4 by 120° counterclockwise. It is important to note that the labels of all variables and all boundary vertices do not rotate; only the orientations of the arrows in Υ change. Consider oriented paths in Υ' from the left side $\{1',2',3',4',5',6'\}$ to the bottom $\{1'',2'',3'',4'',5'',6''\}$. Denote the set of such paths connecting j' to i'' by $\mathfrak{P}^2_{ij}$. Any such path p divides the triangle in two parts: the left part $\widetilde{\mathfrak{B}}^l_p$ containing Z_{600} and the right $\widetilde{\mathfrak{B}}^r_p$ containing Z_{060} and Z_{006}. After restriction $Z_{00n} = Z_{0n0} = Z_{n00} = 1$, we set the weight $w(p) = \prod_{\alpha\in\widetilde{\mathfrak{B}}^l_p} Z_\alpha$, and $(\mathcal{M}_3)_{ij} = \sum_{p\in\mathfrak{P}^2_{ij}} w(p)$. $\mathcal{M}_3$ is upper-triangular.

Next, define the normalized matrices

$$M_i = S \cdot \mathcal{M}_i \cdot D_i^{-1}, \tag{5.1}$$

where

$$D_i = (\det(\mathcal{M}_i))^{1/n} \qquad \text{and} \qquad S = \begin{pmatrix} 0 & \dots & 0 & 1 \\ 0 & \dots & -1 & 0 \\ & \dots & \dots & \\ 0 & (-1)^{n-1} & \dots & 0 \\ (-1)^n & 0 & \dots & 0 \end{pmatrix}.$$

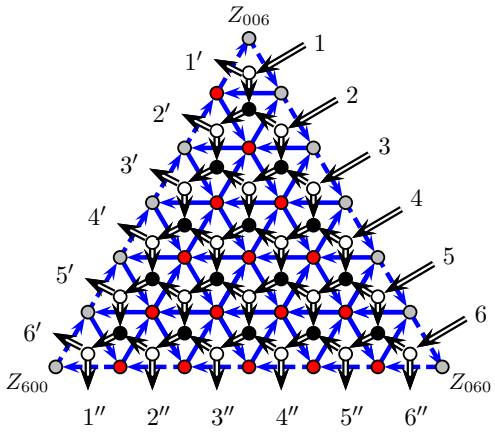


Figure 4. The plabic graph Γ dual to the quiver of Fock–Goncharov parameters.

In [4], it was proposed to set $\widehat{A} = M_1^{\mathsf{T}} M_2$. It is easy to observe that $\widehat{A}$ is upper triangular. Upon normalization discussed below, matrix elements $a_{i,j}$ of $\widehat{A}$ satisfy Poisson relations similar to those satisfied by geodesic functions defined in Section 6. We call $a_{i,j}$ (*generalized*) *geodesic functions*.

The upper-triangular matrix $\widehat{A}$ is constructed from the pair $(\mathcal{M}_1, \mathcal{M}_2)$ thereby defining a Poisson map from the collection of Fock–Goncharov parameters equipped with the Poisson structure $\mathcal{P}_{\mathrm{tr}}$ to the upper-triangular matrices equipped with the symplectic groupoid Poisson bracket $\mathcal{P}_{\mathrm{sym}}$. The expression of a_{ij} in terms of Fock–Goncharov parameters depends neither separately on $Z_{k,0,n-k}$ nor on $Z_{k,n-k,0}$ but only on the product $Z_{k,0,n-k}Z_{n-k,k,0}$ for all $k = 1, \dots, n-1$. Therefore, in the expression of matrix entries a_{ij} parameters $Z_{k,0,n-k}$ and $Z_{n-k,k,0}$ are replaced by their products $Z_{k,0,n-k}Z_{n-k,k,0}$. Replacing a pair of parameters $Z_{k,0,n-k}$ and $Z_{n-k,k,0}$ by their product leads to a new quiver, which is obtained from Γ by the process of *amalgamation*. During the amalgamation, the vertices carrying $Z_{k,0,n-k}$ and $Z_{n-k,k,0}$ are merged into a single vertex carrying $Z_{k,0,n-k}Z_{n-k,k,0}$. The set of arrows incident to the new vertex is the union of arrows incident to either of the two original vertices. The new quiver obtained by amalgamation of all the pairs $Z_{k,0,n-k}$ and $Z_{n-k,k,0}$ for $k = 1, \dots, n-1$ has $n-1$ fewer vertices. The amalgamated quiver has $n-1$ remaining frozen variables $Z_{0,k,n-k}$. The log-canonical Poisson bracket on Z_{ijk} determined by the original quiver induces the log-canonical Poisson bracket for amalgamated parameters determined by the amalgamated quiver. Amalgamation results in the appearance of exactly $n-1$ new independent Casimir functions [4] $\mathfrak{C}_k = \prod_{i=0}^{n-k} Z_{n-k-i,k,i} \cdot \prod_{j=0}^{k} Z_{j,k-j,n-k}$ for all $k = 1, \dots, n-1$. Note that only the first powers of $Z_{ij\ell}$, $i \neq 0$ and exactly one square $Z_{0,k,n-k}^2$, $k = 1, \dots, n-1$ enter $\mathfrak{C}_k$.

After choosing the symplectic leaf $\mathfrak{L} = \{\mathfrak{C}_k = 1\}$ for all $k = 1, \dots, n-1$, any collection of parameters in $\mathfrak{L}$ determines the upper-triangular matrix $\hat{A}$ with *units on the main diagonal*. The *normalizing condition* $\mathfrak{C}_k = 1$ implies

$$Z_{0,k,n-k} = \frac{1}{\sqrt{\prod_{i=0}^{n-k-1} Z_{n-k-i,k,i} \cdot \prod_{j=1}^{k} Z_{j,k-j,n-k}}} \tag{5.2}$$

for $k = 1, \dots, n-1$.

Hence, on the symplectic leaf $\mathfrak{L}$, the frozen parameter $Z_{0,k,n-k}$ can be expressed in terms of the other mutable parameters and is dropped from the set of coordinates.

Remark 5.1. Formula (5.2) explains the appearance of half-integer powers in the expressions for $a_{i,j}$ if $\hat{A}$ satisfies the normalizing condition; see examples in Section 8.

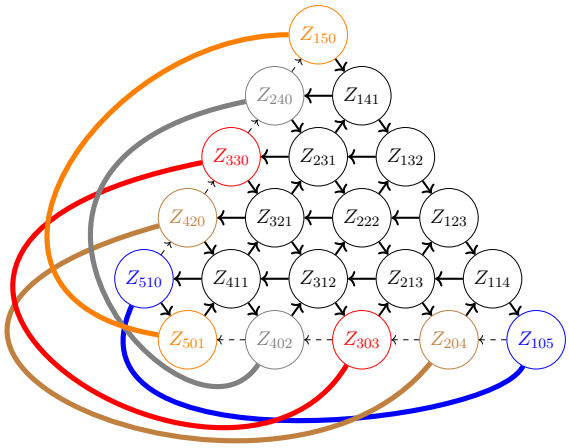


Figure 5. The quiver shows the collection of amalgamated Fock–Goncharov parameters. The amalgamated pairs of variables are shown in the same color and connected by an additional thick curve of the same color. This amalgamated quiver is the one depicted in Figure 25, where parameters a_t, b_t and c_t coincide either with Z_{ijk} or with amalgamated $Z_{k,0,n-k}Z_{n-k,k,0}$.

Remark 5.2. Note that after amalgamation and imposing the normalizing condition, the quiver in Figure 3 becomes the quiver in Figure 5 for the remaining Fock–Goncharov parameters, which is equivalent to the quiver in Figure 25.

6 Geometric leaf and dimension count: The cases $n = 3$ and $n = 4$

We begin by recalling the known parametrization of the Teichmüller space $\mathcal{T}_{g,s}$ of two-dimensional hyperbolic surfaces of genus g with one or two holes. Following [3], for a positive integer $n \geq 3$ consider the following ribbon graph Γ_n consisting of two horizontal chains of $n-3$ equal intervals and n slanted edges connecting vertices of the first chain with vertices of the second chain (see Figure 6 below for $n = 5$).

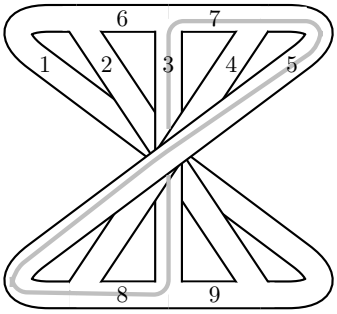


Figure 6. Ribbon graph Γ_5 describes the surface of genus 2 with one hole. The gray curve represents the loop γ_{35}. The matrix of the monodromy operator along the loop γ_{35} is $M_{\gamma_{35}} = L_{x_5}R_{x_8}L_{x_3}R_{x_7}$.

We label the slanted edges 1 through n in left-to-right order of their upper endpoints. Recall, $\mathrm{par}(n) = 1$, for odd n and 2, for even n. Note that the ribbon graph Γ_n is homeomorphic to a surface $\Sigma_{g,s}$ of genus $g = \lfloor \frac{n-1}{2} \rfloor$ with $s = \mathrm{par}(n)$ holes.

The cardinality of the set of edges $E(\Gamma_n)$ of the ribbon graph Γ_n (Figure 6) is $3n-6 = \dim \mathcal{T}_{g,s}$. The collection of positive parameters $x_i = x(e_i) > 0$ for all edges $e_i \in E(\Gamma_n)$, parametrizes the

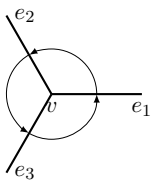


Figure 7. Adjacency indices: $\mathrm{adj}_{\mathbf{v}}(e_1,e_2)=\mathrm{adj}_{\mathbf{v}}(e_2,e_3)=\mathrm{adj}_{\mathbf{v}}(e_3,e_1)=1$; $\mathrm{adj}_{\mathbf{v}}(e_1,e_3)=\mathrm{adj}_{\mathbf{v}}(e_3,e_2)=\mathrm{adj}_{\mathbf{v}}(e_2,e_1)=-1$.

Teichmüller space $\mathcal{T}_{g,s}$ that carries the renowned Goldman Poisson bracket. Parameters x_i are *log-canonical coordinates* for the Goldman bracket

$$\{x_i,x_j\}=\mathrm{adj}(e_i,e_j)x_ix_j, \tag{6.1}$$

where $\mathrm{adj}(e_i,e_j)$ is the adjacency index of edges e_i and e_j. Namely, for $e\in E(\Gamma_n)$ we denote by ∂e the subset $\{P,Q\}$ of two (possibly, coincident) vertices of e; i.e., elements of the set $V(\Gamma_n)$ of vertices of Γ_n such that e connects P and Q.

$$\mathrm{adj}(e_i,e_j)=\sum_{\mathbf{v}\in\partial e_i\cap\partial e_j}\mathrm{adj}_{\mathbf{v}}(e_i,e_j),$$

and the local adjacency index

$$\mathrm{adj}_{\mathbf{v}}(e_i,e_j)=\begin{cases}+1 & \text{if at vertex } \mathbf{v} \text{ the half-edge } e_j \text{ immediately follows } e_i\\ & \text{in the anti-clockwise direction,}\\ -1 & \text{if at vertex } \mathbf{v} \text{ the half-edge } e_j \text{ immediately follows } e_i\\ & \text{in the clockwise direction}\end{cases}$$

(see Figure 7).

Note that adjacency index $\mathrm{adj}(e_i,e_j)$ is well-defined for any pair of edges of a ribbon graph R having only 3-valent vertices. We use it to associate with R a quiver $\mathfrak{Q}_R$ with $|E(R)|$ vertices, called the *geometric quiver*. The vertices are in one-to-one correspondence with edges of R. The number of arrows from vertex e_i to vertex e_j equals $\mathrm{adj}(e_i,e_j)$ if $\mathrm{adj}(e_i,e_j)>0$.

A path in Γ_n is a sequence $P_1,P_2,\dots,P_m$ of vertices such that each pair of consecutive vertices P_i, P_{i+1} is joined by an edge of Γ_n. A path is a loop if $P_m=P_1$. We call a path (or loop) *simple* if there are no repeated edges in the path.

We denote by γ_{ij} the simple loop whose starting point is the top vertex of the slanted edge i, followed by the bottom vertex of slanted i, followed by the simple path of bottom vertices from the bottom vertex of i to the bottom vertex of j, followed by the top vertex of slanted j, followed by the simple path of top vertices from the top vertex of j to the top vertex of i (see Figure 6). Note that γ_{ij} is completely determined by the choice of a pair of indices $1\le i,j\le n$. Note that γ_{ii} is the identity in $\pi_1(\Gamma_n)$ as a trivial loop.

For any closed geodesic path (a loop, possibly with self-intersections) γ in a hyperbolic surface Σ^h, we denote by $M_\gamma\in\mathrm{PSL}_2(\mathbb{R})$ the corresponding deck transformation-isometry of the universal cover $\mathbb{H}$. The geodesic function is given by $G_\gamma=|\mathrm{tr}(M_\gamma)|$. Note that the absolute value of the trace is well-defined for an element of $\mathrm{PSL}_2(\mathbb{R})$.

The *Goldman Poisson bracket* for geodesic functions of two loops α and β intersecting once takes the following form:

$$\{G_\alpha,G_\beta\}=\frac{1}{2}G_{\alpha\beta}-\frac{1}{2}G_{\alpha\beta^{-1}} \tag{6.2}$$

(see Figure 8).

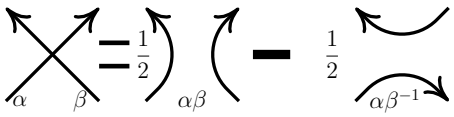


Figure 8. Goldman Poisson bracket.

Definition 6.1. $G_{ij} = |\operatorname{tr} M_{\gamma_{ij}}|$ is the geodesic function corresponding to γ_{ij}, where $M_{\gamma_{ij}} \in \mathrm{PSL}_2(\mathbb{R})$ is the element of the Fuchsian group determined by the loop γ_{ij}.

Remark 6.2. As mentioned above, $G_{ij} = e^{\ell_{ij}/2} + e^{-\ell_{ij}/2}$, where ℓ_{ij} is the geodesic length of γ_{ij}. From the formulas of Section 3, it is easy to find the expression for G_{ij} in terms of parameters x_i. The pushforward of the Goldman bracket (6.2) coincides with the Bondal Poisson bracket on the unipotent triangular matrices $\mathcal{A}_n$ induced from the symplectic groupoid.

Remark 6.3. Note that the graph Γ_n is centrally symmetric. This central symmetry generates the group $\mathbb{Z}_2$. Any slanted edge of Γ_n is centrally symmetric, and any edge in the top horizontal part of Γ_n is centrally symmetric to the corresponding edge of the bottom horizontal part. For instance, each of edges 1–5 in Figure 6 is centrally symmetric, edges 6 and 9 form a centrally symmetric pair, edges 7 and 8 form the other centrally symmetric pair. Therefore, $\mathbb{Z}_2$ acts on $E(\Gamma_n)$ by exchanging edges in all pairs of two distinct centrally symmetric edges. This action induces $\mathbb{Z}_2$-action on the corresponding Teichmüller space $\mathcal{T}_{g,s}$ and on the set of loops in Γ_n.

This $\mathbb{Z}_2$-action on the set of loops changes the orientation of any loop γ_{ij} to the opposite one. Since the geodesic function G_{ij} does not depend on the orientation of the loop γ_{ij}, G_{ij} is invariant under $\mathbb{Z}_2$-action.

Definition 6.4. A Poisson subalgebra of a Poisson algebra $\mathcal{A}$ is a vector subspace of $\mathcal{A}$ closed under multiplication and Poisson bracket. A Poisson subalgebra is generated by a subset S if it is a minimal Poisson subalgebra containing S.

Let $\mathbf{R}_n$ be the Poisson subalgebra generated by $\{G_{ii+1}\}_{1\le i<n}$. Let $\mathcal{O}[\mathcal{T}_{g,s}]^{\mathbb{Z}_2} \subset \mathcal{O}[\mathcal{T}_{g,s}]$ be the subring of $\mathbb{Z}_2$-invariant functions of the ring of regular functions on $\mathcal{T}_{g,s}$. Remark 6.3 implies the following statement.

Lemma 6.5. $\mathbf{R}_n \subseteq \mathcal{O}[\mathcal{T}_{g,s}]^{\mathbb{Z}_2}$.

The Chekhov–Fock map $\varphi\colon \mathcal{T}_{g,s} \to \mathcal{A}_n$ was defined in [3] as follows. For a point $\Sigma^h \in \mathcal{T}_{g,s}$, denote by $G_{ij}(\Sigma^h)$ the value of the geodesic function G_{ij} at Σ^h. Then,

$$\varphi(\Sigma^h) = \begin{pmatrix} 1 & & G_{ij}(\Sigma^h) \\ & \ddots & \\ 0 & & 1 \end{pmatrix}.$$

Recall the following statement.

Theorem 6.6 ([3]). *The map $\varphi\colon \mathcal{T}_{g,s} \to \mathcal{A}_n$ is a Poisson morphism that sends the Goldman Poisson bracket on the Teichmüller space to the Bondal Poisson bracket on the space of the unipotent upper-triangular matrices.*

It was shown in [3] that for a special choice of the geodesics $G_{i,j}$ shown in Figure 6, applying the skein and Poisson relations (the Goldman bracket), a Poisson algebra generated by the finite set $G_{i,j}$, $1 \le i < j \le n$, becomes closed. This algebra of geodesic functions was first obtained by Nelson, Regge, and Zertuche [15] and is also known as the (semiclassical) reflection equation algebra, or twisted Yangian.

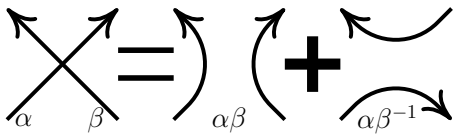


Figure 9. Two paths α and β intersect at one point as shown on the left. The product of the traces of corresponding monodromy operators satisfies the skein relation $\operatorname{tr}(M_\alpha)\operatorname{tr}(M_\beta) = \operatorname{tr}(M_\alpha M_\beta) + \operatorname{tr}\big(M_\alpha M_\beta^{-1}\big) = \operatorname{tr}(M_{\alpha\beta}) + \operatorname{tr}(M_{\alpha\beta^{-1}})$. Notice that path $\alpha\beta$ is isotopic to the first path on the right-hand side and the path $\alpha\beta^{-1}$ is isotopic to the second one.

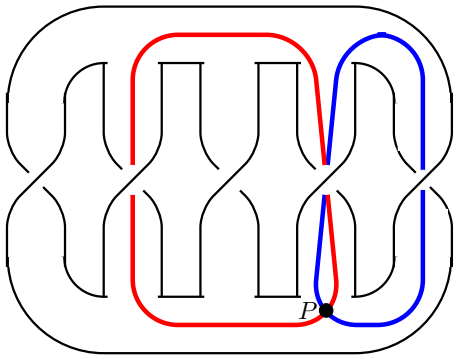


Figure 10. The twisted ribbon graph $\widetilde{\Gamma}_n$ for $n = 5$. The red curve is the loop γ_{24}. The blue curve is the loop γ_{45}. The two loops intersect at point P.

It is well-known that $\dim(\mathcal{T}_{g,s}) = |E(\Gamma_n)| = 3n-6$, (recall that $g = \lfloor \frac{n-1}{2} \rfloor$, $s = \operatorname{par}(n)$) while $\dim(\mathcal{A}_n) = \frac{1}{2}n(n-1)$. The number of independent Casimirs for $\mathcal{T}_{g,s}$ is s and the number of independent Casimirs for $\mathcal{A}_n$ is $\lfloor \frac{n}{2} \rfloor$.

For the case $n = 3$, $\dim(\mathcal{T}_{1,1}) = \dim(\mathcal{A}_3) = 3$. Both $\mathcal{T}_{1,1}$ and $\mathcal{A}_3$ have one Casimir. Therefore, the dimension of a generic symplectic leaf in $\mathcal{T}_{1,1}$ and in $\mathcal{A}_3$ is equal to 2. Moreover, any loop in this case is a sequence of $\mathbb{Z}_2$-invariant arcs and is $\mathbb{Z}_2$-(anti-)symmetric. This observation shows that any geodesic function on $\mathcal{T}_{1,1}$ is $\mathbb{Z}_2$-invariant. (Recall that any elliptic curve has $\mathbb{Z}_2$-symmetry.) For $n > 3$ (equivalently, $s > 1$ or $g > 2$), there exist non-$\mathbb{Z}_2$ (anti-)invariant loops and, hence, non-$\mathbb{Z}_2$ invariant geodesic functions.

Corollary 6.7. $\mathbf{R}_3 \cong \mathcal{O}[\mathcal{T}_{1,1}]$. *For* $n > 3$, $\mathbf{R}_n \subsetneq \mathcal{O}[\mathcal{T}_{g,s}]$.

For the next step, let us recall the *skein relation*: for any two SL_2 matrices A and B one has

$$\operatorname{tr}(A)\operatorname{tr}(B) = \operatorname{tr}(AB) + \operatorname{tr}\big(AB^{-1}\big).$$

(see Figure 9).

Theorem 6.8. $\mathbf{R}_n \cong \mathcal{O}[\mathcal{T}_{g,s}]^{\mathbb{Z}_2}$.

The proof of Theorem 6.8 occupies the rest of this section.

For convenience, we redraw the ribbon graph Γ_n (Figure 6 for $n = 5$) as a homeomorphic *twisted ribbon graph* $\widetilde{\Gamma}_n$ (see Figure 10).

Remark 6.9. The surface of the twisted ribbon graph $\widetilde{\Gamma}_5$ in Figure 10 is homeomorphic to the surface of the ribbon graph Γ_5 in Figure 6. Similarly, surfaces $\widetilde{\Gamma}_n$ are defined that are homeomorphic to Γ_n.

Remark 6.10. A collection of loops $\gamma_1, \dots, \gamma_m$ in $\widetilde{\Gamma}_n$ corresponds to the monomial $\prod_{\alpha=1}^{m} G_{\gamma_\alpha}$. The algebra of geodesic functions has an additive spanning set consisting of monomials corresponding to collections of loops. The skein relation expresses the geodesic function of a loop with self-intersections as a polynomial in geodesic functions of the loops with fewer self-intersections. By induction, we conclude that the algebra of geodesic functions has a spanning set consisting only of monomials corresponding only to collections of nonintersecting loops (laminations).

Note that the isotopy class of any oriented loop in $\widetilde{\Gamma}_n$ is entirely described by the cyclically ordered sequence of an even number of vertical intervals traversed alternately upward and downward in the loop path. We denote by $\widehat{i}$ (correspondingly, $\underset{\smile}{i}$) the directed upwards (correspondingly, directed downwards) interval along the ith vertical edge of $\widetilde{\Gamma}_n$. For instance, the red loop in Figure 10 travelled clockwise corresponds to the sequence $\widehat{2}\underset{\smile}{4}$ (or, equivalently, $\underset{\smile}{4}\widehat{2}$) while the red loop travelled counterclockwise corresponds to the sequence $\underset{\smile}{2}\widehat{4}$ (equivalently, $\widehat{4}\underset{\smile}{2}$). Note that any sequence describing a loop in $\widetilde{\Gamma}_n$ has interlacing overhat and underhat indices. Therefore, such sequence is entirely determined by the direction of the first index in the sequence. Reversing the orientation of the loop interchanges all overhats and underhats and reverses the cyclic order of the sequence. We will denote the oriented closed loop by the sequence of indices, with the first index oriented up or down as $(\widehat{i_1}i_2 \dots i_{2k-1}i_{2k})$. The corresponding geodesic function is denoted $G(\widehat{i_1}i_2 \dots i_{2k-1}i_{2k})$. Recall that the geodesic function does not depend on the orientation of the loop. If reversing the orientation of the sequence produces the sequence in the same cyclic equivalence class as the original sequence, then the change from underhat to overhat and vice versa will not change the geodesic function. In this situation, we will omit the overhat (underhat) if it does not lead to confusion. In particular, $G(i_1i_2) = G(\widehat{i_1}i_2) = G(\underset{\smile}{i_1}i_2)$. Similarly, $G(i_1i_2i_3i_2) = G(\widehat{i_1}i_2i_3i_2) = G(\underset{\smile}{i_1}i_2i_3i_2)$.

To avoid ambiguity, we note that in the class of sequences up to cyclic permutations, there is a unique lexicographically minimal sequence, which we will use to label the corresponding loop.

Lemma 6.11. *For all $1 \le i < j \le n$, $G_{ij} = G(ij) \in \mathbf{R}_n$ and for all $1 \le i < j < k \le n$ elements $G(ijkj), G(ijik), G(ikjk) \in \mathbf{R}_n$.*

Proof. For any $1 \le i_1 < i_2 < i_3 \le n$, the skein relation implies $G(i_1i_2) \cdot G(i_2i_3) = G(i_1i_3) + G(i_1i_2i_3i_2)$. Note that the loops (i_1i_2) and (i_2i_3) intersect exactly in one point implying that $\{G(i_1i_2), G(i_2i_3)\} = \frac{1}{2}G(i_1i_3) - \frac{1}{2}G(i_1i_2i_3i_2)$ by (6.2). Introduce $\langle\langle f, g\rangle\rangle := \frac{1}{2}f \cdot g + \{f, g\}$. Observe that $\langle\langle G(i_1i_2), G(i_2i_3)\rangle\rangle = G(i_1i_3)$, hence, $G(i_1i_3) \in \mathbf{R}_n$. That immediately implies that $G(ijkj) \in \mathbf{R}_n$. Similarly, $G(ijik), G(ikjk) \in \mathbf{R}_n$. ■

Remark 6.12. For an algebra $\mathbb{A}$, we consider its quadratic extension $\mathbb{A}[\xi]$, where ξ is a root of a quadratic polynomial that is irreducible over $\mathbb{A}$, $p(\xi) = a_0 + a_1\xi + a_2\xi^2$, $a_i \in \mathbb{A}$, $p(\xi) = 0$.

Lemma 6.13. *For $1 \le i_1 < i_2 < i_3 < i_4 \le n$, the algebra $\mathbf{R}_n[G(\widehat{i_1}i_2i_3i_4)]$ is a quadratic extension of $\mathbf{R}_n$.*

Proof. Let $f = G(\widehat{i_1}i_2i_3i_4)$, $g = G(\underset{\smile}{i_1}i_2i_3i_4)$ and $\sigma_1 = f + g$ and $\sigma_2 = fg$ be the two elementary symmetric functions of f and g. Construct an unipotent upper-triangular 4×4 matrix U with $U_{st} = G(i_si_t) \in \mathbf{R}_n$ for all $1 \le s < t \le 4$. Coefficient of the first power of λ of $\det\bigl(U + \lambda U^{\mathsf{T}}\bigr)$ coincides with σ_1. The Pfaffian of the skew-symmetric matrix $U - U^{\mathsf{T}}$ is

$$\operatorname{Pf}\bigl(U - U^{\mathsf{T}}\bigr) = \sqrt{\det\bigl(U - U^{\mathsf{T}}\bigr)}$$

and $\sigma_1 = \operatorname{Pf}\bigl(U - U^{\mathsf{T}}\bigr)$. Then, $\sigma_1, \sigma_2 \in \mathbf{R}_n$. It remains to notice that $f, g \notin \mathbf{R}_n$. ■

Corollary 6.14. $G(\underset{\smile}{i_1}i_2i_3i_4) \in \mathbf{R}_n[G(\widehat{i_1}i_2i_3i_4)]$ *and* $G(\widehat{i_1}i_2i_3i_4) \in \mathbf{R}_n[G(\underset{\smile}{i_1}i_2i_3i_4)]$.

Proof. As in the proof of Lemma 6.13, $\sigma_1 \in \mathbf{R}_n$, which implies the statement. ■

Let $\mathcal{R}_n = \mathbf{R}_n[G(\widehat{1}234)]$.

Lemma 6.15. *For all $1 \le i_1 < i_2 < i_3 < i_4 \le n$ both $G(\widehat{i_1}i_2i_3i_4)$ and $G(\underset{\smile}{i_1}i_2i_3i_4)$ belong to $\mathcal{R}_n$.*

Proof. For $k_4 > i_4$, $\langle\langle G(\widehat{i_1}i_2i_3i_4), G(i_4k_4)\rangle\rangle = G(\widehat{i_1}i_2i_3k_4)$. Since $G(i_4k_4) \in \mathbf{R}_n$, we obtain that $G(\widehat{i_1}i_2i_3i_4)$ and $G(\widehat{i_1}i_2i_3k_4)$ either both belong or not belong to $\mathcal{R}_n$ simultaneously. We claim a similar statement for $G(\widehat{i_1}i_2i_3i_4)$ and $G(\widehat{i_1}i_2k_3i_4)$ if $i_3 < k_3 < i_4$; $G(\widehat{i_1}i_2i_3i_4)$ and $G(\widehat{i_1}k_2i_3i_4)$ if $i_2 < k_2 < i_3$; and $G(\widehat{i_1}i_2i_3i_4)$ and $G(\widehat{k_1}i_2i_3i_4)$ if $k_1 < i_1$. Combining all these statements above with the fact that $G(\widehat{1}234) \in \mathcal{R}_n$, we conclude that $G(\widehat{i_1}i_2i_3i_4) \in \mathcal{R}_n$. By Corollary 6.14, we see also that $G(\underset{\smile}{i_1}i_2i_3i_4) \in \mathcal{R}_n$. ■

Lemma 6.16. *The following statements hold:*

(1) *For all $1 \le i_1 < i_2 < i_3 < i_4 < i_5 \le n$, $G(\widehat{i_1}i_3i_5i_4i_3i_2) \in \mathcal{R}_n$.*

(2) *For all $1 \le i_1 < i_2 < i_3 < i_4 < i_5 < i_6 \le n$, $G(\underset{\smile}{i_1}i_2i_3i_4i_5i_6) \in \mathcal{R}_n$. Similarly, $G(\widehat{i_1}i_2i_3i_4i_5i_6) \in \mathcal{R}_n$.*

(3) *For all $1 \le i_1 < i_2 < i_3 < i_4 < i_5 < i_6 \le n$, $G(\underset{\smile}{i_1}i_2i_3i_6i_5i_4) \in \mathcal{R}_n$. Equivalently, $G(\widehat{i_1}i_6i_5i_4i_3i_2) \in \mathcal{R}_n$.*

Proof. (1) Using the skein relations, we see that $2G(\widehat{i_1}i_4i_3i_2)\cdot G(i_3i_5) - 2G(\widehat{i_1}i_5i_3i_2)\cdot G(i_3i_4) = G(\widehat{i_1}i_3i_5i_4i_3i_2) + G(\widehat{i_1}i_5i_3i_4i_3i_2) - G(\widehat{i_1}i_5i_4i_2) - G(\widehat{i_1}i_5i_3i_4i_3i_2) = G(\widehat{i_1}i_3i_5i_4i_3i_2) - G(\widehat{i_1}i_5i_4i_2)$.

Therefore, $G(\widehat{i_1}i_3i_5i_4i_3i_2) = 2G(\widehat{i_1}i_4i_3i_2)\cdot G(i_3i_5) - 2G(\widehat{i_1}i_5i_3i_2)\cdot G(i_3i_4) + G(\widehat{i_1}i_5i_4i_2)$. It remains to notice that the right-hand side of the last equality belongs to $\mathcal{R}_n$ by Lemmas 6.11 and 6.15.

(2) $G(i_1i_2i_3i_4i_5i_6) = -2G(\underset{\smile}{i_1}i_2i_4i_6)\cdot G(i_3i_5) + \frac{1}{2}G(\underset{\smile}{i_1}i_2i_3i_6)\cdot G(i_4i_5) + \frac{1}{2}G(\underset{\smile}{i_1}i_2i_5i_6)\cdot G(i_3i_4) + \{G(i_3i_5), G(\underset{\smile}{i_1}i_2i_4i_6)\}$. By Lemmas 6.11–6.15, the right-hand side belongs to $\mathcal{R}_n$. The second statement is proved similarly.

(3) $G(i_1i_2i_3i_6i_5i_4) = G(\underset{\smile}{i_1}i_2i_3i_4)\cdot G(i_5i_6) + G(\underset{\smile}{i_1}i_2i_3i_6)\cdot G(i_4i_5) - G(\underset{\smile}{i_1}i_2i_3i_4i_5i_6) - G(\underset{\smile}{i_1}i_2i_3i_5)\cdot G(i_4i_6)$. The right-hand side belongs to $\mathcal{R}_n$ by Lemmas 6.11–6.15 above and part (2). ■

Definition 6.17. We call the union of two disconnected horizontal intervals of $\widetilde{\Gamma}_n$ between vertical edge i and $i+1$ *gate i*. We say that a simple loop in $\widetilde{\Gamma}_n$ is *horizontally 2-bounded* if it travels every gate and every vertical edge at most twice: at most once in one direction and at most once in the opposite direction.

We say that a simple loop in $\widetilde{\Gamma}_n$ is *2-bounded* if it travels every edge (vertical and horizontal) at most twice: at most once in one direction and at most once in the opposite direction.

Lemma 6.18. *If γ is a simple horizontally 2-bounded loop in $\widetilde{\Gamma}_n$ then $G_\gamma \in \mathcal{R}_n$.*

Proof. The proof follows the arguments of Lemmas 6.15 and 6.16 for loops with a longer tail. ■

Lemma 6.19. *Let γ be a simple 2-bounded loop that travels once left-to-right along the bottom horizontal legs in gates $i-1$ and i, once right-to-left along the top horizontal legs in the same gates and does not travel along the vertical edge i (as shown in Figure 11). Denote by γ_L (or, γ_R) the shortened left (or, right) part of γ (as shown in Figure 12). If both G_{γ_L} and G_{γ_R} belong to $\mathcal{R}_n$, then $G_\gamma \in \mathcal{R}_n$.*

Proof. As in the proof of Lemma 6.11, it is enough to notice that $\langle\langle G_{\gamma_L}, G_{\gamma_R}\rangle\rangle = G_\gamma$. ■

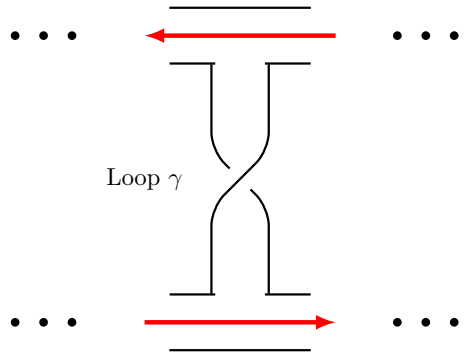


Figure 11. The simple closed loop γ (in red) skips the vertical leg i.

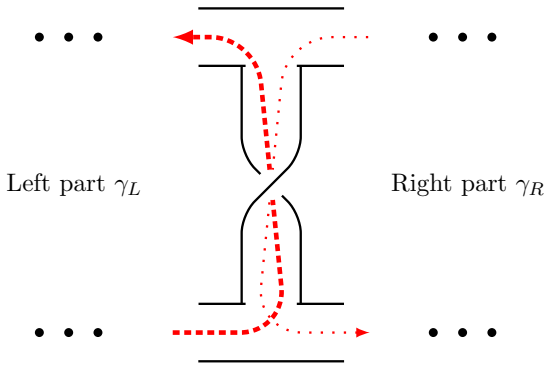


Figure 12. The left part γ_L is thick dashed, the right part γ_R is thin dotted.

Remark 6.20. Note a simple 2-bounded loop that skips vertical leg i and travels once along the top and the bottom horizontal legs of gates i and $i+1$ must travel along the top and bottom horizontal legs in the opposite directions, otherwise it cannot be a closed loop.

Definition 6.21. We call a simple 2-bounded loop *maximal* if it travels every edge exactly twice: once in each direction.

Lemma 6.22. *For all odd $n \geq 3$, a maximal simple 2-bounded loop in $\widetilde{\Gamma}_n$ is either* $(\widehat{1}\ 2\ 3\ \ldots n-1\ n\ 1\ 2 \ldots n-1\ n)$ *or* $(\underset{\smile}{1}\ 2\ 3\ \ldots n-1\ n\ 1\ 2 \ldots n-1\ n)$

Proof. By inspection. ■

Corollary 6.23. *A maximal simple 2-bounded loop exists only for odd n. For even n, both sequences of indices in Lemma 6.22 lead to two connected components.*

Lemma 6.24. *If n is odd and γ is the maximal loop then $G_\gamma \in \mathbf{R}_n$.*

Proof. Let

$$G_{123\ldots n} = G_{12}G_{23}G_{34}\ldots G_{n-1,n}G_{1n}, \qquad G^{(2)} = \sum_{1\leq i<j\leq n} G_{ij}^2,$$

$$G^{(3)} = \sum_{1\leq i<j<k\leq n} G_{ij}G_{jk}G_{ik}, \qquad G^{(4)} = \sum_{1\leq i<j<k<l\leq n} G_{ij}G_{jk}G_{kl}G_{il},$$

etc. Define the nth Markov function $\mathcal{M}^{(n)}$ on $\mathcal{T}_{g,s}$ as follows:

$$\mathcal{M}^{(n)} = G_{123\ldots n} - G^{(n-1)} + G^{(n-2)} - \cdots + (-1)^n G^{(2)} + (-1)^{n+1}2(2-n) \in \mathbf{R}_n.$$

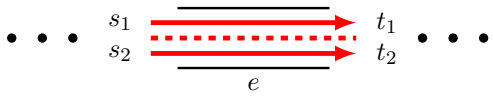


Figure 13. An edge traveled twice in the same direction.

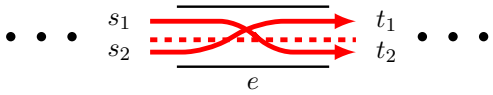


Figure 14. Crossing the edges travelled in the same direction.

For odd n, the $\mathbb{Z}_2$-symmetry reverses the orientation of the loop $(\widehat{1}\ 2\ 3\ \ldots n{-}1\ n\ 1\ 2\ldots n{-}1\ n)$, implying equality $G(\widehat{1}\ 2\ 3\ \ldots n-1\ n\ 1\ 2\ldots n-1\ n) = G(\widehat{1}\ 2\ 3\ \ldots n-1\ n\ 1\ 2\ldots n-1\ n)$. Repeatedly applying the skein relation to the product $G_{12}G_{23}G_{34}\ldots G_{n-1,n}G_{1n}$ and all products in $G^{(k)}$, $k=2,\ldots,n-1$, we observe that $G(\widehat{1}\ 2\ 3\ \ldots n-1\ n\ 1\ 2\ldots n-1\ n) = \mathcal{M}^{(n)}$. ■

Lemma 6.25. *For any simple 2-bounded loop γ, its geodesic function G_γ belongs to $\mathcal{R}_n$.*

Proof. The claim follows from Lemmas 6.18, 6.19, and 6.24. ■

Remark 6.26. Any simple non-2-bounded loop in $\widetilde{\Gamma}_n$ has at least one edge that it travels twice in the same direction (segments $s_1 \to t_1$ and $s_2 \to t_2$ in Figure 13 both run in the same direction along the ribbon edge e). Other segments of the same loop may run either between segments $s_1 \to t_1$ and $s_2 \to t_2$ or above or below in either direction, as the dashed one in Figure 13. Since both $s_1 \to t_1$ and $s_2 \to t_2$ are nonintersecting segments of the same simple loop γ, this loop follows from s_1 to t_1, then to s_2, then to t_2, and then returns to s_1.

Theorem 6.27. *For any simple loop γ, its geodesic function G_γ belongs to $\mathcal{R}_n$.*

Proof. For each edge e of the ribbon graph we define the *lane number* of e in γ as $\ell_e(\gamma) = \max(0, r_{\overleftarrow{e}}(\gamma) - 1) + \max(0, r_{\overrightarrow{e}}(\gamma) - 1)$ where $r_{\overleftarrow{e}}(\gamma)$ is the number of times γ travels e in one direction while $r_{\overrightarrow{e}}(\gamma)$ is the number of times γ travels e in the opposite direction. Define *the total lane number* of γ as $\ell(\gamma) = \sum_e \ell_e(\gamma)$ where the sum is over all edges of $\widetilde{\Gamma}_n$.

We prove the statement by induction on $\ell(\gamma)$.

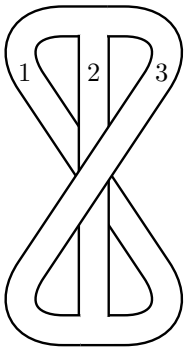
Lemma 6.25 is the base case of the induction because $\ell(\gamma) = 0$ if and only if γ is a 2-bounded simple loop.

For the induction step, we consider e as in Figure 13. Note that if we replace segments $s_1 \to t_1$ and $s_2 \to t_2$ by the crossed segments $s_1 \to t_2$ and $s_2 \to t_1$ as in Figure 14, we obtain two intersecting loops γ_1 and γ_2 (not necessarily simple). Then we can use the skein relation for the product $G_{\gamma_1} \cdot G_{\gamma_2}$ to obtain the sum of two geodesic functions of (possibly, nonsimple) loops: one is γ and the second $\tilde{\gamma}$ whose total lane number is strictly smaller $\ell(\tilde{\gamma}) < \ell(\gamma)$. It remains to notice that $\ell(\gamma_1) < \ell(\gamma)$ and $\ell(\gamma_2) < \ell(\gamma)$ and also that resolving a crossing using the skein relation does not increase the total lane number. Therefore, we express G_γ through $G_{\gamma_1}, G_{\gamma_2}$ and $G_{\tilde{\gamma}}$ with these geodesic functions belonging to $\mathcal{R}_n$ by the induction assumptions.

That completes the proof of Theorem 6.27. ■

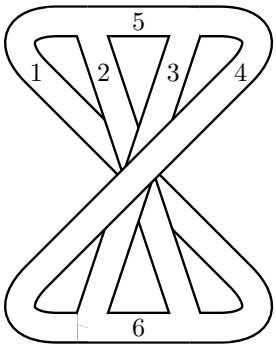
Now we are ready to prove Theorem 6.8.

Proof of Theorem 6.8. Theorem 6.27 and Remark 6.10 imply that the geodesic function of any loop is in the quadratic extension $\mathcal{R}_n$ of $\mathbf{R}_n$. Let P be a quadratic polynomial in $\mathbf{R}_n[x]$ with roots ρ_1 and ρ_2 such that $\mathcal{R}_n = \mathbf{R}_n[\rho_1] = \mathbf{R}_n[\rho_2]$. $\mathbb{Z}_2$-action permutes the roots ρ_1 and ρ_2. In view of Lemma 6.13, elementary symmetric functions of ρ_1 and ρ_2 belong to $\mathbf{R}_n$. It implies that $\mathbf{R}_n$ coincides with the $\mathbb{Z}_2$-invariant subalgebra $\mathcal{O}[\mathcal{T}_{g,s}]^{\mathbb{Z}_2}$ ■



$$\begin{bmatrix} 1 & G_{12} & G_{13} \\ 0 & 1 & G_{23} \\ 0 & 0 & 1 \end{bmatrix}$$

Figure 15. $n = 3$. Edge k is assigned an exponential shear parameter x_k. See Figure 2.



$$\begin{bmatrix} 1 & G_{12} & G_{13} & G_{14} \\ 0 & 1 & G_{23} & G_{24} \\ 0 & 0 & 1 & G_{34} \\ 0 & 0 & 0 & 1 \end{bmatrix}$$

Figure 16. $n = 4$. Edge k is assigned an exponential shear parameter x_k.

Since $\mathcal{T}_{g,s}$ is a union of isomorphic symplectic leaves and, by Theorem 6.8, φ is a 2-to-1 Poisson map, $\mathrm{Im}(\varphi)$ is a union of symplectic leaves of the same dimension in $\mathcal{A}_n$. Moreover, if for $s = 2$ we consider a generic (not containing fixed points of $\mathbb{Z}_2$-action) geometric symplectic leaf of the Bondal Poisson structure in $\mathcal{A}_n$ it is locally isomorphic to the generic symplectic leaf of $\mathcal{T}_{g,s}$.

Definition 6.28. We call $\mathrm{Im}(\varphi)$ a *geometric locus*. A *geometric symplectic leaf* is a generic symplectic leaf in the geometric locus.

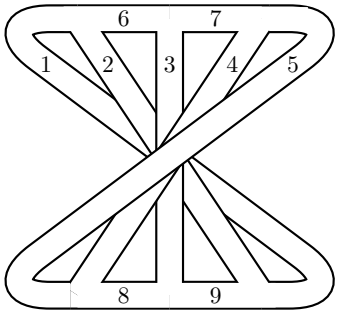
We now consider low dimensional cases. For $n = 3$, $\dim(\mathcal{T}_{1,1}) = \dim(\mathcal{A}_3) = 3$. For $n = 4$, $\dim(\mathcal{T}_{1,2}) = \dim(\mathcal{A}_4) = 6$.

If $n = 3$ or $n = 4$, since the dimensions coincide, $\mathrm{Im}(\varphi)$ is a subset of $\mathcal{A}_n$ of maximal dimension. The dimension of a generic symplectic leaf in $\mathcal{T}_{1,2}$ and in $\mathcal{A}_4$ is 4. The maps from the clusters of $\mathcal{A}_3$ and $\mathcal{A}_4$ quivers to the clusters in the corresponding Teichmüller spaces are identities since both $\mathcal{A}_3$ and $\mathcal{A}_4$ quivers coincide with the quivers in Teichmüller spaces. Therefore, the positivity condition merely requires all $\mathcal{A}_3$ and $\mathcal{A}_4$ cluster variables to be positive.

For $n \geq 5$, $\dim(\mathcal{T}_{g,s}) < \dim(\mathcal{A}_n)$. For example, for $n = 5$, $\dim(\mathcal{T}_{2,1}) = 9$ and $\dim(\mathcal{A}_5) = 10$. $\mathrm{Im}(\varphi)$ is a subvariety of $\mathcal{A}_5$ of codimension 1. The dimensions of generic symplectic leaves in $\mathcal{T}_{2,1}$ and in $\mathcal{A}_5$ still coincide, and are equal to 8.

For $n \geq 6$, the dimension of a generic symplectic leaf in $\mathcal{T}_{g,s}$ is strictly less than that of a generic symplectic leaf in $\mathcal{A}_n$.

Remark 6.29. In the cases above, the functions G_{ij} are functions of the exponential shear parameters x_k of the edges k of the ribbon graphs in Figures 15–17.



$$\begin{bmatrix} 1 & G_{12} & G_{13} & G_{14} & G_{15} \\ 0 & 1 & G_{23} & G_{24} & G_{25} \\ 0 & 0 & 1 & G_{34} & G_{35} \\ 0 & 0 & 0 & 1 & G_{45} \\ 0 & 0 & 0 & 0 & 1 \end{bmatrix}$$

Figure 17. $n = 5$. Edge k is assigned an exponential shear parameter x_k.

7 Description of pre-geometric leaf: Rank condition

In this and the next sections, we set aside the positivity condition, concentrating on the necessary rank condition.

For

$$A = \begin{pmatrix} 1 & & & G_{ij} \\ & 1 & & \\ & & \ddots & \\ 0 & & & 1 \end{pmatrix} \in \mathrm{Im}(\varphi),$$

we have

$$A + A^{\mathsf{T}} = \begin{pmatrix} 2 & & & G_{ij} \\ & 2 & & \\ & & \ddots & \\ G_{ij} & & & 2 \end{pmatrix}.$$

Note that γ_{ii} is a contractible loop. Hence $G_{ii} = 2$ and we can replace the ith diagonal element of $A + A^{\mathsf{T}}$ by G_{ii} for $1 \le i \le n$.

We write

$$A + A^{\mathsf{T}} = \begin{pmatrix} G_{11} & & & G_{ij} \\ & G_{22} & & \\ & & \ddots & \\ G_{ji} & & & G_{nn} \end{pmatrix},$$

where $G_{ji} = G_{ij}$.

Choose points S_1 and S_2 in a fat graph as shown in Figure 18. For any i, we introduce the holonomy operator $F_i \in \mathrm{SL}_2(\mathbb{R})$ defined as a product of elementary matrices along the path connecting S_1 to S_2 and containing edge i, as drawn in Figure 18. The monodromy is $M_{\gamma_{ij}} = F_j^{-1} F_i$.

Definition 7.1. Define a map from $\mathrm{SL}_2 \times \mathrm{SL}_2$ to $\mathbb{R}$ by

$$(A, B) := \mathrm{tr}\big(B^{-1}A\big).$$

Note that SL_2 is a subset of the linear space of 2×2 real matrices $\mathrm{Mat}_{2\times 2} \cong \mathbb{R}^4$ whose linear span is $\mathrm{Mat}_{2\times 2}$. Since $\det(B) = 1$, the operator $B \mapsto B^{-1}$ is a restriction of a linear operator $\mathrm{Mat}_{2\times 2} \to \mathrm{Mat}_{2\times 2}$ implying that $(\bullet, \bullet)$ allows an extension to a bilinear $\mathbb{R}$-valued form on $\mathrm{Mat}_{2\times 2}$. By an abuse of notation, we also denote the bilinear form by $(\bullet, \bullet)$.

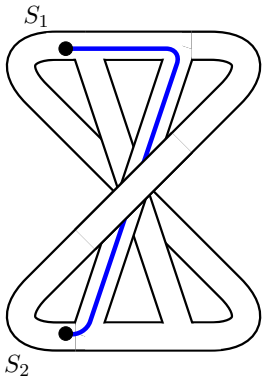


Figure 18. Path corresponding to $F_3 = LX(x_5)RX(x_3)R$.

For $A, B, C \in \mathrm{SL}_2$, $\alpha, \beta \in \mathbb{R}$, we have

- $(A, B) = \mathrm{tr}\big(B^{-1}A\big) = \mathrm{tr}\big(A^{-1}B\big) = (B, A)$.
- $(\alpha A + \beta B, C) = \mathrm{tr}\big(C^{-1}(\alpha A + \beta B)\big) = \alpha \mathrm{tr}\big(C^{-1}A\big) + \beta \mathrm{tr}\big(C^{-1}B\big) = \alpha(A, C) + \beta(B, C)$.
- $(A, A) = \mathrm{tr}\big(A^{-1}A\big) = \mathrm{tr}(\mathrm{Id}) = 2$.

Hence the bilinear form $\langle \cdot, \cdot \rangle$ restricted to $\mathrm{SL}_2 \times \mathrm{SL}_2$ is a restriction of the inner product on $\mathrm{Mat}_{2\times 2}$. The (i, j)-th entry of the matrix $A + A^{\mathsf{T}}$ is $\mathrm{tr}\big(F_j^{-1}F_i\big) = (F_i, F_j)$, i.e., $A + A^{\mathsf{T}}$ is the Gram matrix of inner products (F_i, F_j).

Recall that the Gram matrix of n vectors $\mathbf{v}_1, \ldots, \mathbf{v}_n$ in m-dimensional space $\mathbb{R}^m$ equipped with a bilinear form $\big(\bullet, \bullet\big)$ is $H = (h_{ij})_{i,j=1}^n$ with $h_{ij} = \big(\mathbf{v}_i, \mathbf{v}_j\big)$.

The following classical statement is well known.

Lemma 7.2. $\mathrm{rank}(H) \leq m$.

Since all F_i, $i = 1, \ldots, n$ are vectors in $M_{2\times 2} \cong \mathbb{R}^4$, by the previous lemma, $\mathrm{rank}\big(A + A^{\mathsf{T}}\big) \leq 4$.

This proves the following condition on the matrix A (see [14, 15]).

Corollary 7.3 (rank condition)**.** *If* $A \in \mathrm{Im}(\varphi)$*, then* $\mathrm{rank}\big(A + A^{\mathsf{T}}\big) \leq 4$.

Conjecture 7.4. We conjecture that a positivity condition (described explicitly for $n = 5, 6$ in the next sections) and the rank condition are necessary and sufficient for A to belong to the geometric locus.

The results of this paper imply that the conjecture holds for $n \leq 6$.

8 Solving the rank condition

The strategy of verifying Conjecture 7.4 is as follows: we consider all possible solutions of the rank condition in the $\mathcal{A}_n$ quiver with cluster variables (x_α), transforming them, if necessary, using standard mutations to a new quiver with cluster variables $(\widetilde{x}_\beta)$. The rank condition becomes a system of equations $f_m(\widetilde{x}_\beta) = 0$. Constraints f_m are Lagrangian (of the first kind) because the rank condition is coisotropic. We then resolve the rank condition on the set of geodesic functions $G_{i,j}(\widetilde{x}_\beta)$ and show that these functions can be written in terms of new coordinates (y_γ) (in all cases of nontrivial reduction, the number of y's is strictly smaller than the number of $\widetilde{x}_\beta$), that is, $G_{i,j}(\widetilde{x}_\beta) = G_{i,j}(y_\gamma(\widetilde{x}_\beta))$. The new variables $y_\gamma(\widetilde{x}_\beta)$ possess a Poisson structure induced by that of $\widetilde{x}_\beta$. If Poisson relations for y_γ's are given by equation (6.1), for some ribbon graph of the genus $\lfloor \frac{n-1}{2} \rfloor$ with $\mathrm{par}(n)$ holes then $G_{i,j}(y_\gamma)$ become geodesic functions from Section 3.

8.1 Expressing the rank condition in terms of transport matrices

For a generic unipotent upper-triangular matrix A_n, $\operatorname{rank}\big(A_n+A_n^{\mathsf{T}}\big)=n$. If $\operatorname{corank}\big(A_n+A_n^{\mathsf{T}}\big)\geq 1$, then $\det\big(A_n+A_n^{\mathsf{T}}\big)=0$. The following *groupoid condition* was shown in [4]:

$$M_2=M_3M_1,$$

where M_i, D_i and S are defined by equation (5.1).

Using that $\hat{A}_n=M_1^{\mathsf{T}}M_2$, it was observed in [5] that

$$\begin{aligned}\hat{A}_n&=M_1^{\mathsf{T}}M_2=M_1^{\mathsf{T}}M_3M_1=(S\mathcal{M}_1)^{\mathsf{T}}(S\mathcal{M}_3)(S\mathcal{M}_1)\big(D_1^2D_3\big)^{-1}\\&=\mathcal{M}_1^{\mathsf{T}}\big(S^{\mathsf{T}}S\big)\mathcal{M}_3S\mathcal{M}_1\big(D_1^2D_3\big)^{-1}=\mathcal{M}_1^{\mathsf{T}}\mathcal{M}_3S\mathcal{M}_1\big(D_1^2D_3\big)^{-1},\\\hat{A}_n+\hat{A}_n^{\mathsf{T}}&=\big(D_1^2D_3\big)^{-1}\big(\mathcal{M}_1^{\mathsf{T}}\mathcal{M}_3S\mathcal{M}_1+\mathcal{M}_1^{\mathsf{T}}S^{\mathsf{T}}\mathcal{M}_3\mathcal{M}_1\big)\\&=\big(D_1^2D_3\big)^{-1}\big(\mathcal{M}_1^{\mathsf{T}}\big(\mathcal{M}_3S+S^{\mathsf{T}}\mathcal{M}_3^{\mathsf{T}}\big)\mathcal{M}_1\big).\end{aligned}$$

Since $\mathcal{M}_1$ is nondegenerate, and D_1 and D_3 are nonzero,

$$\operatorname{rank}\big(\hat{A}_n+\hat{A}_n^{\mathsf{T}}\big)=\operatorname{rank}(\Psi),\tag{8.1}$$

where

$$\Psi:=\mathcal{M}_3S+S^{\mathsf{T}}\mathcal{M}_3^{\mathsf{T}}$$

is a lower anti-triangular matrix

8.2 $n=3$ or 4

In these two cases, the rank condition (Corollary 7.3) holds automatically because $n\leq 4$. Moreover, the quivers $\mathcal{A}_3$ and $\mathcal{A}_4$ coincide with the quivers in Teichmüller spaces. They are the quivers associated with ribbon graphs for genus-one surfaces with one and two holes, respectively. The geometric locus is also characterized by the positivity condition. The positivity condition in both cases requires that all cluster variables in $\mathcal{A}_3$ ($\mathcal{A}_4$, correspondingly) are positive.

8.3 $n=5$

When $n=5$, the rank condition holds if and only if $\det\big(A_5+A_5^{\mathsf{T}}\big)=0$. By (8.1), this means that at least one of the anti-diagonal terms of the matrix Ψ must be zero. Let $(-1)^k m_{k,6-k}$, $k=1,\dots,5$ be anti-diagonal terms of $\mathcal{M}_3S$. Recall that in Section 5 the entries of $\mathcal{M}_3$ are expressed in terms of Z_{ijk} or, equivalently, in terms of cluster parameters $b_1=Z_{401}Z_{140}$, $b_2=Z_{131}$, $b_3=Z_{122}$, $b_4=Z_{113}$, $b_5=Z_{104}Z_{410}$, $a_1=Z_{311}$, $a_2=Z_{302}Z_{230}$, $a_3=Z_{221}$, $a_4=Z_{212}$, $a_5=Z_{203}Z_{320}$ assigned to the vertices of the amalgamated quiver in Figure 21. Let us recall now that all antidiagonal terms of $\mathcal{M}_3S$ are monomials in $a_1,\dots,a_5,b_1,\dots,b_5$ and $\Psi^{\mathsf{T}}=\Psi$.

In particular, we distinguish the following three cases depending on the position of the vanishing anti-diagonal element of Ψ:

(0) $2m_{33}=0$. This case is empty because m_{33} is a monomial in cluster variables a_i, b_j and we assume that cluster variables never vanish;

(1) $m_{2,4}+m_{4,2}=m_{2,4}(1+C_1)=0$, where $C_1=\prod_{i=1}^5 a_i$. In this case, the rank condition is equivalent to the equation $C_1=-1$.

(2) $m_{1,5}+m_{5,1}=m_{1,5}(1+C_1C_2)=0$, where C_1 is as above and $C_2=\prod_{i=1}^5 b_i$. In this case, the rank condition becomes $C_1C_2=-1$.

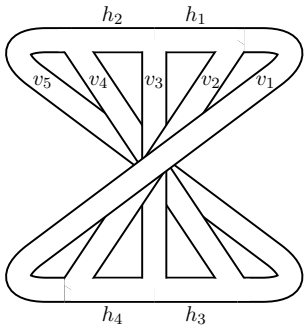


Figure 19. The labeled ribbon graph for $n = 5$.

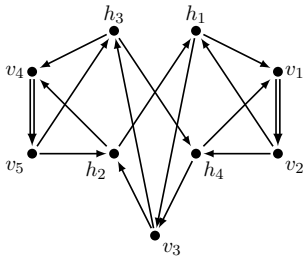


Figure 20. Quiver for $\mathcal{T}_{2,1}$.

A geometric cluster quiver for $\mathcal{T}_{2,1}$ can be obtained from the ribbon graph in Figure 19. To simplify further formulas, we denote the exponential shear parameters of horizontal and slanted edges in Figure 19 by different letters.

The Goldman Poisson structure is described by a geometric quiver as explained in Section 6. Each edge of the ribbon graph in Figure 19 corresponds to a vertex of the quiver (Figure 20) via equation (6.1). An arrow of the quiver connects two edges a to b that share a common endpoint if b immediately follows a under rotation in the anticlockwise direction about the common endpoint.

The log-canonical parameters for the Poisson variety $\mathcal{A}_n$ were built in [4] by modifying the Fock–Goncharov construction. The quiver of the corresponding Poisson structure is obtained by amalgamating and removing certain vertices from the quiver describing Fock–Goncharov parameters for $n = 5$, similar to one on Figure 3, as explained in Section 5. The result is the quiver on Figure 21 for $\mathcal{A}_5$ (a corresponding quiver for $\mathcal{A}_6$ is shown on Figure 5).

8.3.1 Coisotropic reduction in case (1)

We now describe the procedure that relates the quiver in Figure 21 with the quiver in Figure 20 under the condition that $C_1 = -1$. Note that the number of vertices of the first quiver is 10, while the number of vertices of the second quiver is 9. This indicates that this procedure must include a coisotropic reduction.

Let us introduce the following notation. For any $z_1, z_2, \dots, z_n$, let

$$\langle z_1 z_2 \cdots z_{n-1} z_n \rangle := (z_1 z_2 \cdots z_{n-1} z_n)^{\frac{1}{2}} \times \left(1 + \frac{1}{z_1} + \frac{1}{z_1 z_2} + \cdots + \frac{1}{z_1 z_2 \cdots z_{n-1}} + \frac{1}{z_1 z_2 \cdots z_{n-1} z_n}\right).$$

Let $\hat{A}_5$ be the unipotent 5×5 matrix constructed from the original $\mathcal{A}_5$-quiver in Figure 21,

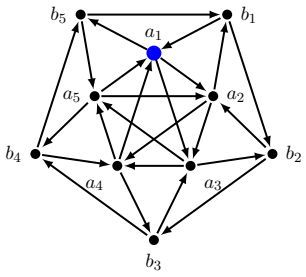


Figure 21. Exchange quiver of the cluster structure for $\mathcal{A}_5$ describing the Poisson bracket in log-canonical coordinates.

and let a_{ij} be its ij-th entry. As discussed at the end of Section 5, we obtain uniform expressions:

$$a_{1,2} = \langle b_1 a_1 a_3 b_2 \rangle, \qquad a_{2,3} = \langle b_2 a_2 a_4 b_3 \rangle, \qquad a_{3,4} = \langle b_3 a_3 a_5 b_4 \rangle, \qquad a_{4,5} = \langle b_4 a_4 a_1 b_5 \rangle. \tag{8.2}$$

Remark 8.1. Note that in both the $\mathcal{A}_n$ and geometric cases, elements $a_{i,i+1} (= G_{i,i+1})$ with $1 \leq i < n$ generate the full set of matrix elements using Poisson and skein relations: for any $i < j < k$, $a_{i,k} = \{a_{i,j}, a_{j,k}\} + \frac{1}{2} a_{i,j} a_{j,k}$, so, starting with $a_{i,i+1}$, we can consecutively construct all other $a_{i,k}$.

Remark 8.2. The expressions of all $a_{i,j}$ are universal Laurent polynomials; i.e., they retain their polynomial forms upon all sequences of mutations. This is true for all matrix elements in all $\mathcal{A}_n$ quivers. For a general $\mathcal{A}_n$-quiver having a form similar to that in Figures 21 and 25, the generating matrix elements $a_{i,i+1}$ are given by $a_{i,i+1} = \langle x_i y_{i_1} z_{j_1} w_{k_1} \cdots w_{k_2} z_{j_2} y_{i_2} x_{i+1} \rangle$, where x_i and x_{i+1} are cluster variables of the "outer" layer of the $\mathcal{A}_n$ quiver (the corresponding vertices are of order four) connected by an arrow $x_i \to x_{i+1}$. All cluster variables in this sequence form a directed path in $\mathcal{A}_n$ quiver:

$$x_i \to y_{i_1} \to z_{j_1} \to w_{k_1} \to \cdots \to w_{k_2} \to z_{j_2} \to y_{i_2} \to x_{i+1},$$

and the path is the shortest path that passes through all layers of the quiver and includes exactly two variables of each layer except the innermost layer for which it includes two variables for odd n and one variable for even n.

Note that in the cases $n = 3$ and $n = 4$, the image $\mathrm{Im}(\varphi)$ is an open subset in $\mathcal{A}_n$. One can check that, in this case, the geodesic functions can be written uniquely in terms of (square roots of) log-canonical parameters. The relation to the corresponding cluster variables of $\mathcal{A}_3$ and $\mathcal{A}_4$ was presented in [4].

In case (1) for $n = 5$, we proceed by performing a cluster mutation μ_{a_1} at the large highlighted blue vertex a_1, followed by mutations μ_{a_4} at a_4 and μ_{a_3} at a_3, which yields the following quiver (see Figure 22).

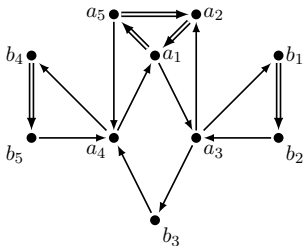


Figure 22. Quiver for $\mathcal{A}_5$ after cluster mutation.

In the next step of the transformation, we make a coisotropic reduction. To do it, we compute the geodesic functions $G_{i,j}$ for $\mathcal{T}_{2,1}$ and compare them with the corresponding generalized geodesic functions $a_{i,j}$ in $\mathcal{A}_5$. We express geodesic functions G_{ij} in terms of shear coordinates of the ribbon graph in Figure 19 (or, equivalently, in terms of quiver variables in Figure 20). We collect them in the right-hand side of (8.3).

Rewriting expressions (8.2) after the mutations $\mu_{a_4}\mu_{a_3}\mu_{a_1}$ (the order of mutations is right to left) of the cluster in Figure 21, we obtain the expressions for $a_{i,i+1}$ in terms of a_i, b_i parameters of quiver in Figure 22 and collect them in the left-hand side of the following system:

$$\begin{aligned}
a_{1,2} &= \langle b_1 b_2\rangle = \langle v_1 v_2\rangle = G_{1,2},\\
a_{2,3} &= \langle b_2 a_3 a_2 a_1 a_3 b_3\rangle\\
&= (v_2 h_4 h_1 v_3)^{\frac12}\left(1+\frac{1}{v_2}+\frac{1}{h_1 v_2}+\frac{1}{h_4 v_2}+\frac{1}{h_4 h_1 v_2}+\frac{1}{v_3 h_4 h_1 v_2}\right) = G_{2,3},\\
a_{3,4} &= \langle b_3 a_4 a_1 a_5 a_4 b_4\rangle\\
&= (v_3 h_2 h_3 v_4)^{\frac12}\left(1+\frac{1}{v_3}+\frac{1}{v_3 h_3}+\frac{1}{v_3 h_2}+\frac{1}{v_3 h_2 h_3}+\frac{1}{v_3 h_2 h_3 v_4}\right) = G_{3,4},\\
a_{4,5} &= \langle b_4 b_5\rangle = \langle v_4 v_5\rangle = G_{4,5}, \qquad C_1 = a_1 a_2 a_5, \qquad C_2 = \prod_{i=1}^{5} b_i a_3^2 a_4^2 a_1.
\end{aligned} \tag{8.3}$$

We wish to find expressions for v_i, h_i in terms of a_j, b_j that make (8.3) hold (a solution is clearly not unique: although, in $n=5$ case, the number of variables is the same if we take into account the constraint $a_1 a_2 a_5 = -1$, there is an infinite braid-group symmetry that preserves the quiver).

Inspection suggests the substitution

$$v_i = b_i \qquad \text{for all } i \in \{1,2,3,4,5\}. \tag{8.4}$$

Performing this substitution simplifies the equation for $G_{2,3}$ to

$$\left(a_1 a_2 a_3^2\right)^{\frac12}\left(\frac{1}{a_3}+\frac{1}{a_2 a_3}+\frac{1}{a_1 a_2 a_3}+\frac{1}{a_1 a_2 a_3^2}\right) = (h_4 h_1)^{\frac12}\left(\frac{1}{h_1}+\frac{1}{h_4}+\frac{1}{h_1 h_4}\right).$$

This equation holds if the following two conditions are satisfied:

(1) $\left(a_1 a_2 a_3^2\right)^{\frac12} = (h_4 h_1)^{\frac12} \implies h_1 h_4 = a_1 a_2 a_3^2$,

(2) $\dfrac{1}{a_3}+\dfrac{1}{a_2 a_3}+\dfrac{1}{a_1 a_2 a_3}+\dfrac{1}{a_1 a_2 a_3^2} = \dfrac{1}{h_1}+\dfrac{1}{h_4}+\dfrac{1}{h_1 h_4} \implies h_1 + h_4 = a_1 a_2 a_3 + a_1 a_3 + a_3.$

Condition (2) implies the relation $h_4 = a_1 a_2 a_3 + a_1 a_3 + a_3 - h_1$ whose substitution into condition (1) yields the equation

$$h_1(a_1 a_2 a_3 + a_1 a_3 + a_3 - h_1) = a_1 a_2 a_3^2,$$

which becomes the quadratic equation

$$h_1^2 - (a_1 a_2 a_3 + a_1 a_3 + a_3) h_1 + a_1 a_2 a_3^2 = 0.$$

Solving for h_1 and observing that the conditions are symmetric for h_1 and h_4 yields

$$h_1, h_4 = \frac{a_3}{2}\left(a_1 a_2 + a_1 + 1 \pm \sqrt{a_1^2 a_2^2 + 2a_1^2 a_2 - 2a_1 a_2 + a_1^2 + 2a_1 + 1}\right). \tag{8.5}$$

Similar reasoning for G_{34} implies

$$h_2, h_3 = \frac{a_4}{2}\Big(a_1a_5 + a_5 + 1 \pm \sqrt{a_1^2a_5^2 + 2a_1a_5^2 - 2a_1a_5 + a_5^2 + 2a_5 + 1}\Big). \tag{8.6}$$

We claim now that the variables $v_1, \dots, v_5, h_1, \dots, h_4$ given by formulas (8.4), (8.5), (8.6) satisfy Poisson commutation relations determined by the quiver in Figure 20 under the condition that the Casimir function $C_1 = a_1a_2a_5$ of the Poisson bracket defined by the quiver from Figure 22 takes the value -1.

Indeed, clearly, $a_1a_2a_5$ is a Casimir function of the quiver in Figure 22. We are interested in the case where the value of the Casimir function

$$a_1a_2a_5 = -1. \tag{8.7}$$

This critical condition is equivalent to rank condition (Corollary 7.3), the only one we need to make the reduction. To verify the expressions of the v_i and h_j in terms of the b_i and a_j, we seek to verify the commutation relations of the quiver in Figure 20. Note that by construction, $\{v_i, v_j\} = \{b_i, b_j\}$. Note also that all b_i Poisson commute with any variable of $\{a_1, a_2, a_5\}$. Comparing the quivers in Figures 20 and 22, we immediately conclude that the arrows of the quiver in Figure 20 between v_i and v_j and between v_i and h_j reflect correct Poisson relations between corresponding expressions (8.4), (8.5), (8.6).

It remains to check the Poisson commutation relations between h_1, h_2, h_3, h_4. We show first that $\{h_1, h_4\} = 0$. Indeed, $\{h_1 + h_4, h_1h_4\} = (h_1 - h_4)\{h_1, h_4\}$. It remains to notice that $h_1h_4 = a_1a_2a_3^2$, which Poisson-commutes with a_1, a_2 and a_3, hence, with any function of a_1, a_2, a_3. Therefore, $(h_1 - h_4)\{h_1, h_4\} = 0$, because h_1 and h_4 are functions of a_1, a_2 and a_3 only. Since $h_1 - h_4 \neq 0$, we conclude that $\{h_1, h_4\} = 0$. Similarly, we prove that $\{h_2, h_3\} = 0$.

Direct computation shows $\{h_3, h_4\} = h_3h_4$ and, similarly, $\{h_2, h_1\} = h_2h_1$.

Next, we verify that $\{h_2 + h_3, h_1 + h_4\} = \{h_2, h_1\} + \{h_3, h_4\}$. Recall that $a_5 = -\frac{1}{a_1a_2}$ to compute

$$\begin{aligned}
\{h_2, h_1\} + \{h_3, h_4\} &= \frac{a_3a_4}{2}\Big((a_1a_5 + a_5 + 1)(a_1a_2 + a_1 + 1) \\
&\quad \pm \sqrt{((a_1a_5 + a_5 + 1)^2 - 4a_1a_5)\big((a_2a_1 + a_1 + 1)^2 - 4a_1a_2\big)}\Big) \\
&= \frac{a_3a_4}{2}\Big(\Big(-\frac{1}{a_2} - \frac{1}{a_1a_2} + 1\Big)(a_1a_2 + a_1 + 1) \\
&\quad \pm \frac{1}{a_1a_2}\big((a_1a_2 + a_1 + 1)^2 - 4a_1a_2\big)\Big) \\
&= \frac{a_3a_4}{2a_1a_2}\Big(\big(a_1^2a_2^2 - a_1^2 - 2a_1 - 1\big) \\
&\quad + \big(a_1^2a_2^2 + 2a_1^2a_2 + 2a_1a_2 + 2a_1 + a_1^2 + 1 - 4a_1a_2\big)\Big) \\
&= \frac{a_3a_4}{2a_1a_2}\Big(2a_1^2a_2^2 + 2a_1^2a_2 - 2a_1a_2\Big) \\
&= a_3a_4(a_1a_2 + a_1 - 1), \\
\{h_2 + h_3, h_1 + h_4\} &= \{a_4(a_1a_5 + a_5 + 1), a_3(a_1a_2 + a_1 + 1)\} \\
&= \Big\{a_4\Big(-\frac{1}{a_2} - \frac{1}{a_1a_2} + 1\Big), a_3(a_1a_2 + a_1 + 1)\Big\} \\
&= a_4(a_1a_2 + a_1 + 1)\Big\{-\frac{1}{a_2} - \frac{1}{a_1a_2} + 1, a_3\Big\} \\
&\quad + a_3\Big(-\frac{1}{a_2} - \frac{1}{a_1a_2} + 1\Big)\{a_4, a_1a_2 + a_1 + 1\}
\end{aligned}$$

$$
\begin{aligned}
&+ a_3a_4\Big\{-\frac{1}{a_2}-\frac{1}{a_1a_2}+1, a_1a_2+a_1+1\Big\}\\
&= a_4(a_1a_2+a_1+1)\Big(-\frac{a_3}{a_2}\Big)+a_3\Big(-\frac{1}{a_2}-\frac{1}{a_1a_2}+1\Big)(a_1a_2a_4+a_1a_4)\\
&\quad + a_3a_4\Big(2a_1+\frac{2a_1+2}{a_2}\Big)\\
&= a_3a_4\Big(-a_1-\frac{a_1}{a_2}-\frac{1}{a_2}-a_1-\frac{a_1}{a_2}-1-\frac{1}{a_2}\\
&\quad + a_1a_2+a_1+2a_1+\frac{2a_1}{a_2}+\frac{2}{a_2}\Big)\\
&= a_3a_4(a_1a_2+a_1-1).
\end{aligned}
$$

Subtracting the first equation from the second, we obtain

$$\{h_2,h_4\}+\{h_3,h_1\}=0. \tag{8.8}$$

Note that symmetric polynomials of h_1, h_4 and h_2, h_3 are expressible as polynomials in a_1, a_2, a_3 and a_1, a_4, a_5, correspondingly. From such expressions of h_1+h_4 and h_2h_3 and commutation relations for a_i, we easily see that $\{h_1+h_4, h_2h_3\}=(h_1+h_4)h_2h_3$. In particular,

$$\{h_1,h_3\}h_2+\{h_4,h_2\}h_3=0. \tag{8.9}$$

Combining (8.8) and (8.9) and taking into account that the determinant

$$\det\begin{pmatrix}-1 & -1\\ h_2 & h_3\end{pmatrix}=h_2-h_3\neq 0$$

for generic h_2, h_3, we conclude $\{h_2,h_4\}=0$ and $\{h_1,h_3\}=0$.

Therefore, under the rank condition $a_1a_2a_5=-1$ the Poisson bracket between the variables v_1, v_2, v_3, v_4, v_5, h_1, h_2, h_3, h_4 given by (8.4), (8.5), (8.6) is described by the quiver in Figure 20.

We have found an explicit form of the Poisson map $\mathcal{T}_{2,1}\to\mathcal{A}_5$ in terms of coordinates v_i, h_j in Case (1).

Remark 8.3. Note that, unlike higher n cases, for $n=5$ we can invert formulas (8.5) and (8.6) taking condition (8.7) into account and express a_i, $i=1,\dots,5$, in terms of h_j, $j=1,\dots,4$ (see (A.1)). The resulting $a_i(h_j)$ are rational functions, and it is straightforward to check that the homogeneous Poisson relations for variables h_j induce those for $a_i(h_j)$.

8.3.2 Case (2)

Instead of performing reduction directly in this case, we present a procedure that reduces this case to case (1) via invertible sequences of mutations. For this, let us introduce a convenient notation, which we also use in the $n=6$ case.

In any quiver, monomial Casimirs $x_1^{\alpha_1}x_2^{\alpha_2}\cdots x_n^{\alpha_n}$ with integers α_i are determined by null vectors of the exchange matrix B: $B\vec{\alpha}=\vec{0}$. Upon mutation at x_j, $\vec{\alpha}\to\vec{\alpha}'$ with

$$\alpha_i'=\alpha_i \qquad \text{for } i\neq j \qquad \text{and} \qquad \alpha_j'=-\alpha_j+\sum_i B_{i,j}^{(+)}\alpha_i,$$

where the sum ranges over only the positive entries of the matrix B. Note that the nullity condition implies that

$$\sum_i B_{i,j}^{(+)}\alpha_i+\sum_i B_{i,j}^{(-)}\alpha_i=0 \qquad \forall j.$$

Here, $B_{ij}^{(+)} = \max(B_{ij}, 0)$, $B_{ij}^{(-)} = \min(0, B_{ij})$. We leave it as a simple but nice exercise for the reader to check that this condition is preserved under mutations.

We start with the quiver in Figure 21 assigning to each vertex a 2-row vector in which the first component is the power of this variable in the expression for C_1 and the second component is the power of this variable in the expression for C_1C_2. In Figure 23, we show the original quiver and the quiver obtained from it by successive mutations at b_2, b_4, and b_3. Note that the Casimirs C_i preserve monomial form but the powers of mutated cluster variables in the monomial expressions for Casimirs may change because the variables themselves change.

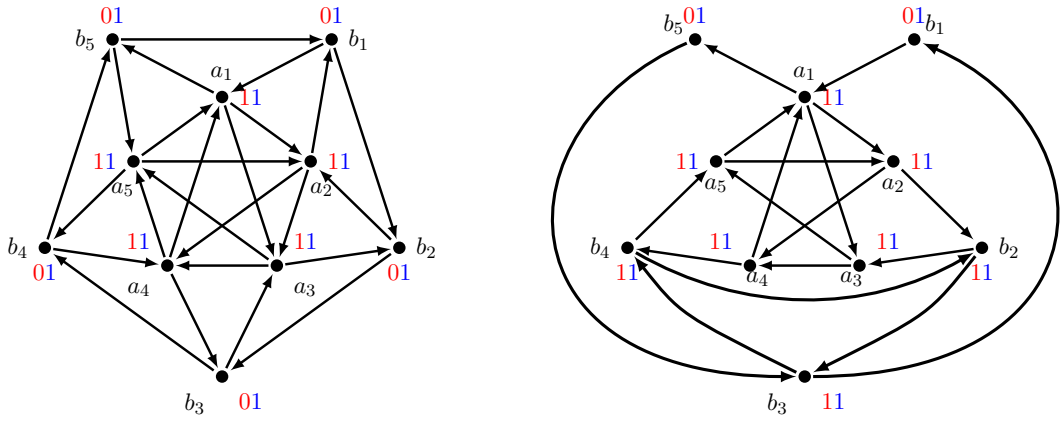


Figure 23. Left: $\mathcal{A}_5$-quiver with powers of Casimirs C_1 and C_2 indicated. Right: the same quiver after mutations at b_4, b_2, and b_3.

The only difference between powers of C_1 and C_1C_2 in the initial quiver (on the left in Figure 23) and in the transformed quiver (on the right) appears at vertices b_1 and b_5. If we now perform mutations at these two vertices and permute variables b_1 and b_5, we obtain the quiver (see Figure 24), which has exactly the same form, except that b_1 switches positions with b_5 and all powers of variables in C_1 and C_1C_2 are interchanged. Performing mutations at b_3, b_2, and b_4 then returns us to the original $\mathcal{A}_5$-quiver with values of C_1 and C_1C_2 interchanged. We can then perform reduction as described in case (1).

Remark 8.4. Despite the fact that for the coisotropic reduction in this section we used the rank condition on the matrix A whose elements G_{ij} are $\mathbb{Z}_2$ invariant, the cluster algebra obtained as the result of the reduction contains, in particular, all exponential shear coordinates as cluster variables and, hence, all geodesic functions (symmetric or not) are universal Laurent polynomials of the square roots of these cluster variables.

8.4 $n = 6$

8.4.1 The rank condition for $n = 6$ and Fock–Goncharov parameters

The rank condition for $n = 6$ claims that $\operatorname{corank}\left(A + A^{\mathsf{T}}\right) = 2$. We now use the fact that the rank condition can be rewritten (8.1) in terms of the matrix $\mathcal{M}_3 S$. Let us denote the elements of the main diagonal of $\mathcal{M}_3$ by $m_{i,i}$ (where i is the row index). Recall that S is anti-symmetric for $n = 6$. Then both $\mathcal{M}_3 S$ and $(\mathcal{M}_3 S)^{\mathsf{T}}$ are lower anti-triangular with entry $(-1)^{i-1} m_{ii}$ in the ith row of the anti-diagonal of $\mathcal{M}_3 S$ and $(-1)^i m_{n-i+1,n-i+1}$ in the ith row of the anti-diagonal of $S^{\mathsf{T}} \mathcal{M}_3^{\mathsf{T}} = (\mathcal{M}_3 S)^{\mathsf{T}}$.

Since the matrix $\mathcal{M}_3 S + S^{\mathsf{T}} \mathcal{M}_3^{\mathsf{T}}$ is symmetric, it contains three pairs of equal anti-diagonal elements $m_{11} - m_{61}$, $-m_{25} + m_{52}$, $m_{34} - m_{43}$. The equation $\det\left(\mathcal{M}_3 S + S^{\mathsf{T}} \mathcal{M}_3^{\mathsf{T}}\right) = 0$ is equivalent

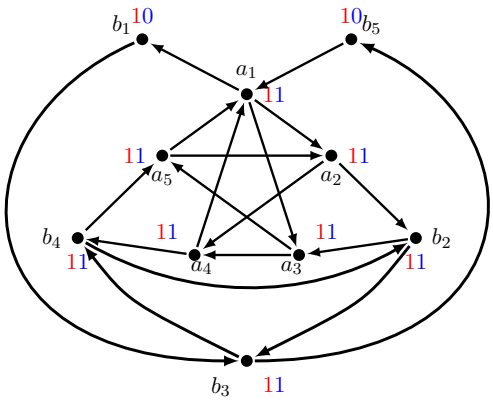


Figure 24. Positions of b_1 and b_5, and exponents of variables in C_1 and C_1C_2 are interchanged.

to the condition (called *Casimir condition*) that at least one of these three anti-diagonal elements vanishes. Introduce the anti-diagonal lower-triangular 6×6 matrix $\Psi = (\psi_{ij})_{i,j=1}^{6}$.

By the reasoning above, the Rank Condition $\operatorname{rank}\bigl(A_6 + A_6^{\mathsf{T}}\bigr) \leq 4$ for $n = 6$ means that $\operatorname{corank}(\Psi) \geq 2$. Corank is at least one when two symmetric elements of the anti-diagonal vanish. To increase the corank by one more, we must require the vanishing of an additional minor. More exactly, the rank condition splits into the following three cases:

1. *Casimir condition* $\psi_{34} = \psi_{43} = 0$ and $\psi_{44} = 0$.
2. *Casimir condition* $\psi_{25} = \psi_{52} = 0$ and $\det\bigl(\Psi_{[3,5]}^{[3,5]}\bigr) = 0$.
3. *Casimir condition* $\psi_{16} = \psi_{61} = 0$ and $\det\bigl(\Psi_{[2,6]}^{[2,6]}\bigr) = 0$.

Rewriting all three cases in terms of variables a_i, b_j, c_k we obtain the following:

Case 1: The Casimir condition is $K_1 = \prod_{j=1}^{3} c_j = 1$. The condition $\psi_{4,4} = 0$ becomes $1 + c_2 + c_2c_3 = 0$.

Case 2: The Casimir condition is $K_2 = \prod_{i=1}^{6} b_i \prod_{j=1}^{3} c_j = 1$. The condition $\det\bigl(\Psi_{[3,5]}^{[3,5]}\bigr) = 0$ is a polynomial containing 108 monomial terms, all with positive signs, which we omit here.

Case 3: The Casimir condition is $K_3 = \prod_{i=1}^{6} a_i b_i \prod_{j=1}^{3} c_j = 1$. The expansion of the function $\det\bigl(\Psi_{[2,6]}^{[2,6]}\bigr)$ contains 3,888 monomials (counted with multiplicities), again, all with positive signs which we omit here.

In the following subsections, we analyze these cases more carefully, beginning with the simplest case, Case 1.

8.4.2 Coisotropic reduction: Case 1

We describe the coisotropic reduction that restores exponential shear coordinates and the Goldman Poisson structure on the geometric leaf in Case 1 of the solution of the rank condition in $\mathcal{A}_6$.

Recall that the amalgamation procedure described in [4] and Section 5 replaces the product $Z_{\ell,0,6-\ell}Z_{6-\ell,\ell,0}$ by one variable because the expression for any geodesic function contains solely the product $Z_{\ell,0,6-\ell}Z_{6-\ell,\ell,0}$ for all $\ell = 1, \ldots, 5$. In particular, the amalgamated coordinates a_1, a_2, a_3, a_4, a_5, a_6, b_1, b_2, b_3, b_4, b_5, b_6, c_1, c_2, c_3 were introduced in [4]. Each a_i, b_i, or c_i is either one of the parameters Z_{ijk} or the product $Z_{\ell,0,6-\ell}Z_{6-\ell,\ell,0}$ such that all entries of $A \in \mathcal{A}_6$ are Laurent polynomial expressions in $a_i^{1/2}$, $b_j^{1/2}$, $c_k^{1/2}$. The Poisson bracket for a_i, b_j, c_k is described by the quiver in Figure 25 (isomorphic to the quiver in Figure 5).

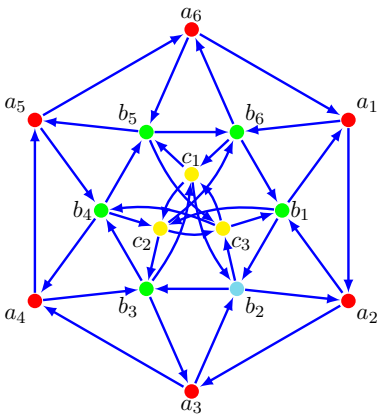


Figure 25. Quiver of the Poisson bracket and cluster structure for $\mathcal{A}_6$.

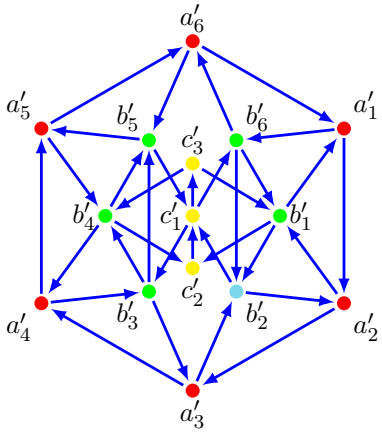


Figure 26. $\mathcal{A}_6$-quiver upon mutation at c_1.

The elementary geodesic functions $G_{i,i+1}$, $i = 1, \dots, 5$, and $G_{6,1}$ are

$$\langle a_6 b_5 c_3 b_1 a_1 \rangle, \qquad \langle a_1 b_6 c_1 b_2 a_2 \rangle, \qquad \langle a_2 b_1 c_2 b_3 a_3 \rangle,$$
$$\langle a_3 b_2 c_3 b_4 a_4 \rangle, \qquad \langle a_4 b_3 c_1 b_5 a_5 \rangle, \qquad \langle a_5 b_4 c_2 b_6 a_6 \rangle.$$

The reduction conditions are

$$c_1 c_2 c_3 = 1 \qquad \text{and} \qquad 1 + \frac{1}{c_2} + \frac{1}{c_2 c_3} = 0.$$

Mutating at c_1, we obtain the transformed $n = 6$ quiver depicted in Figure 26.

In the quiver in Figure 26, the corresponding elementary geodesic functions are

$$\langle a'_6 b'_5 c'_1 c'_3 b'_1 a'_1 \rangle, \qquad \langle a'_1 b'_6 b'_2 a'_2 \rangle, \qquad \langle a'_2 b'_1 c'_2 c'_1 b'_3 a'_3 \rangle,$$
$$\langle a'_3 b'_2 c'_1 c'_3 b'_4 a'_4 \rangle, \qquad \langle a'_4 b'_3 b'_5 a'_5 \rangle, \qquad \langle a'_5 b'_4 c'_2 c'_1 b'_6 a'_6 \rangle.$$

By prime, we denote the corresponding cluster variables after mutations.

Let us rewrite the reduction conditions in the new cluster variables:

$$c_1 c_2 c_3 = 1 \iff \frac{1}{c'_1} c'_2 \frac{c'_1}{1 + c'_1} c'_3 (1 + c'_1) = c'_2 c'_3 = 1,$$
$$1 + \frac{1}{c_2} + \frac{1}{c_2 c_3} = 0 \iff 1 + \frac{1 + c'_1}{c'_2 c'_1} + \frac{1 + c'_1}{c'_1 c'_2 c'_3 (1 + c'_1)}$$

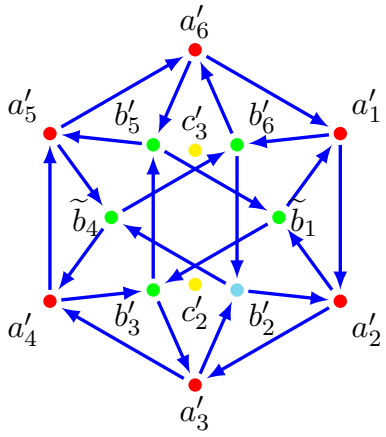


Figure 27. Quiver of the Poisson bracket for variables a'_1, a'_2, a'_3, a'_4, a'_5, a'_6, $\widetilde{b}_1$, b'_2, b'_3, $\widetilde{b}_4$, b'_5, b'_6.

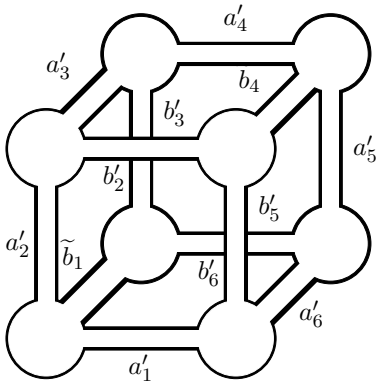


Figure 28. Ribbon graph of a genus-2 surface with 2 holes.

$$= 1 + \frac{1+c'_1}{c'_2c'_1} + \frac{1}{c'_1c'_2c'_3} \overset{c'_2c'_3=1}{=\!=} 1 + \frac{1}{c'_1c'_2} + \frac{1}{c'_2} + \frac{1}{c'_1} = 0 \iff \left(1+\frac{1}{c'_2}\right)\left(1+\frac{1}{c'_1}\right) = 0.$$

We conclude that the reduction conditions become

$$c'_2c'_3 = 1, \qquad \left(1+\frac{1}{c'_1}\right)\left(1+\frac{1}{c'_2}\right) = 0,$$

whose solution is

$$c'_2 = -1, \qquad c'_3 = -1. \tag{8.10}$$

Note that the solution $c'_1 = -1$ is not in the set of allowed values for mutation at c_1.

Consider the expression $\langle a'_6b'_5c'_1c'_3b'_1a'_1\rangle$. Imposing conditions (8.10) and introducing new variables $\widetilde{b}_1 = -c'_1b'_1$, $\widetilde{b}_4 = -c'_1b'_4$, we can write all six geodesic functions as follows: $\langle a'_6b'_5\widetilde{b}_1a'_1\rangle$, $\langle a'_1b'_6b'_2a'_2\rangle$, $\langle a'_2\widetilde{b}_1b'_3a'_3\rangle$, $\langle a'_3b'_2\widetilde{b}_4a'_4\rangle$, $\langle a'_4b'_3b'_5a'_5\rangle$, $\langle a'_5\widetilde{b}_4b'_6a'_6\rangle$.

Amalgamating $-b'_1c'_1 = \widetilde{b}_1$ and $-b'_4c'_1 = \widetilde{b}_4$, we obtain a new quiver, in which c'_2 and c'_3 are detached because they Poisson-commute with all the variables obtained after amalgamation.

Note that all vertices of the quiver (Figure 27) are four-valent with two incoming arrows and two outgoing arrows. It is straightforward to check that this quiver corresponds to a ribbon graph (Figure 28) for $g = 2$, $s = 2$ with vertices of the quiver corresponding to edges of the ribbon graph.

The geodesic functions take the form

$$\operatorname{tr}(R_{a'_1}L_{\widetilde{b}_1}L_{b'_5}L_{a'_6}),\qquad \operatorname{tr}(R_{a'_2}L_{b'_2}L_{b'_6}L_{a'_1}),\qquad \operatorname{tr}(R_{a'_3}L_{b'_3}L_{\widetilde{b}_1}L_{a'_2}),$$
$$\operatorname{tr}(R_{a'_4}L_{\widetilde{b}_4}L_{b'_2}L_{a'_3}),\qquad \operatorname{tr}(R_{a'_5}L_{b'_5}L_{b'_3}L_{a'_4}),\qquad \operatorname{tr}(R_{a'_6}L_{b'_6}L_{\widetilde{b}_4}L_{a'_5}).$$

Remark 8.5. Note that condition (8.10) indicates that c'_2 and c'_3 do not belong to the set of allowed values for mutations at c'_2 and c'_3.

8.4.3 Coisotropic reduction: Cases 2 and 3

Instead of trying to construct a straightforward coisotropic reduction for Cases 2 and 3, we use an indirect approach which we already used in the case $n = 5$. More precisely, we find sequences of mutations that transform Cases 2 and 3 to Case 1. Note that the cases differ in which elements of Ψ vanish. The vanishing of the corresponding elements corresponds to setting the value of the corresponding Casimir function K_1, K_2, or K_3 equal to 1 as explained above. Each Casimir function is a monomial in the variables a_i, b_i, and c_i that are assigned to the vertices of the quiver in Figure 25. We assign to every variable a 3-row vector in $\mathbb{Z}^3$, whose components are the exponents of the corresponding variable in the respective Casimir functions. In the figures below, the red color corresponds to exponents in K_1, the green to K_2, and the blue to K_3. In the following figure, we see that $K_1 = c_1c_2c_3$, and so on.

We observe first that the mutation sequences below permute the Casimir functions of the quiver in Figure 25. Then we check that the sequences permute the corresponding minors $\psi_{4,4}$, $\det\big(\Psi^{[3,5]}_{[3,5]}\big)$, and $\det\big(\Psi^{[2,6]}_{[2,6]}\big)$. Beginning with the quiver for $\mathcal{A}_6$, we perform the following mutations at the bold highlighted vertices. Under the mutations, K_1, K_2, and K_3 remain monomials of mutated variables whose exponents are the components of vectors written in Figure 29.

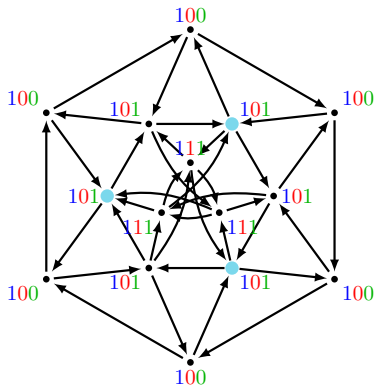


Figure 29. Exponents of variables in expressions of K_1, K_2, and K_3 are written as vectors with colored entries.

The result is shown in Figure 30. We continue with the sequence of mutations at the bold highlighted vertices.

This yields the following quiver depicted in Figure 31.

The triples of numbers near each vertex encode the corresponding Casimir function: red numbers correspond to the smallest Casimir function (Case 1), green numbers correspond to the intermediate Casimir function (Case 2), and blue numbers encode the Casimir function of Case 3. More precisely, the Casimir function is obtained as the product of cluster variables raised to the power indicated by the number printed in the corresponding color.

The last quiver above can be redrawn as the next quiver depicted in Figure 32.

Now consider the following sequence of mutations performed on one of the "wings" of this quiver (see Figure 33). Since we only mutate the bottom three vertices of the quiver, we

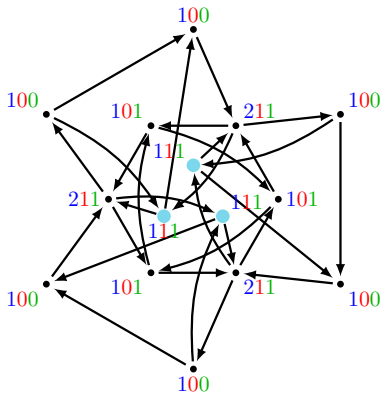


Figure 30. Result of three commuting mutations at the fat lightblue vertices of the quiver in Figure 29.

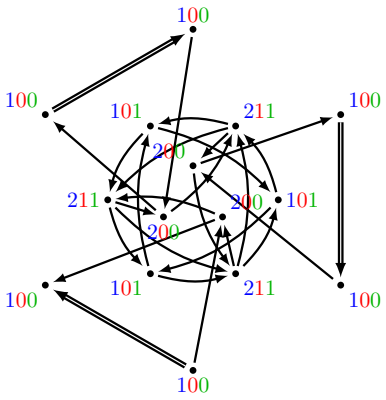


Figure 31. Result of three commuting mutations at the fat lightblue vertices of the quiver in Figure 30.

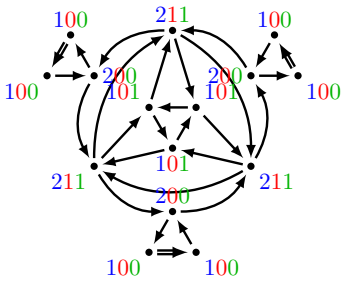


Figure 32. This quiver is equivalent to the quiver in Figure 31.

need consider only those vertices and their neighbors (the highlighted region). Applying these mutations to all three wings of the quiver yields the quiver depicted in Figure 34.

We are done with mutations of the wings, and now turn our attention to the highlighted area depicted in Figure 35.

We now present a sequence of mutations on this quiver that interchanges the first and third Casimirs (see Figure 36). Observe that the Casimirs of Cases 1 and 3 are interchanged in the final two quivers. Thus, relabeling the two most recently mutated vertices and repeating the sequence of mutations that led to this second-to-last quiver in reverse returns us to the original quiver, but with the Casimirs of Cases 1 and 3 interchanged.

Next, in Figure 37 we present a sequence of vertex swaps that cyclically permutes the Casimirs.

If we now relabel two pairs of variables, we obtain the starting quiver (1) with the Casimirs of Cases 1, 2 and 3 permuted cyclically in that order. Repeating now the sequence of mutations

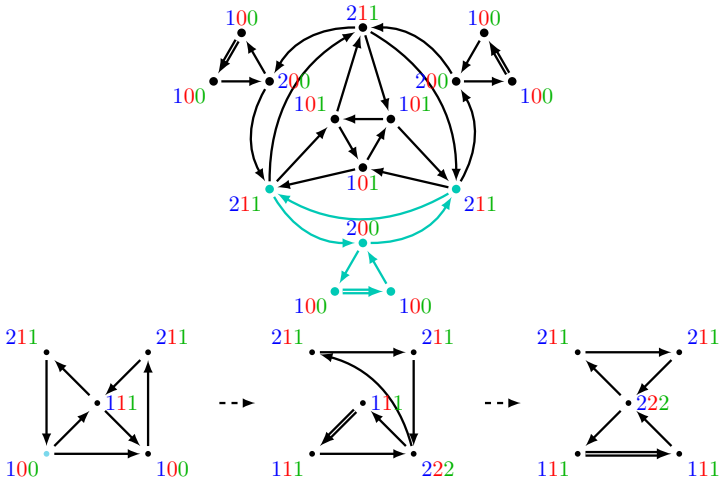


Figure 33. Three consecutive mutations at the vertices of the bottom highlighted triangle in the cyclic counterclockwise order starting from the top vertex.

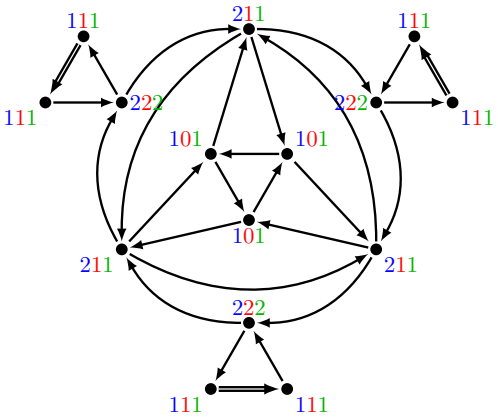


Figure 34. Result of the three sequences of mutations from Figure 33 applied to all three triangles (wings) of the quiver in Figure 33.

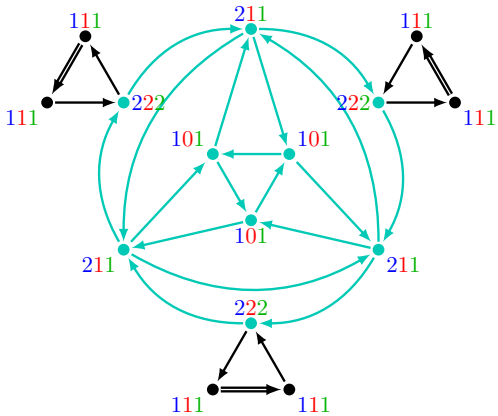


Figure 35. Subsequent mutation sequences are located inside the highlighted area.

in reverse, we obtain the original $\mathcal{A}_6$-quiver with two pairs of relabeled vertices and with all three Casimirs cyclically permuted.

Straightforward verification using MAPLE confirms the following statement.

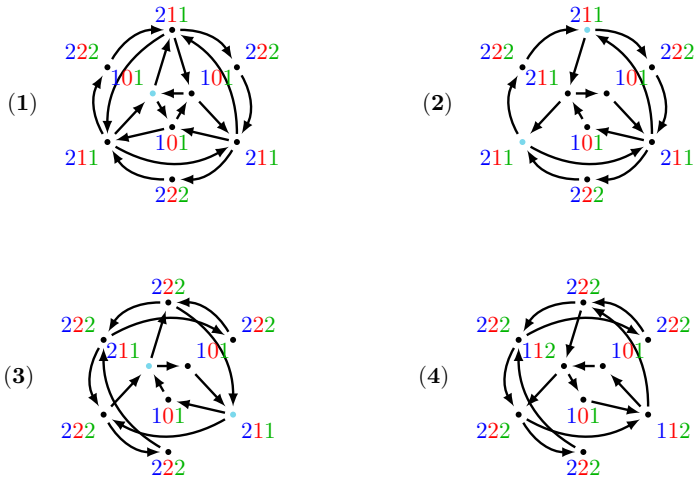


Figure 36. A mutation sequence that interchanges the first and third Casimirs.

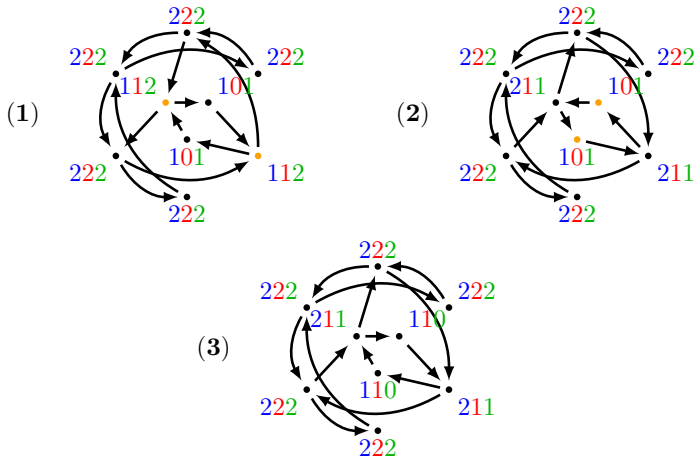


Figure 37. A mutation sequence that cyclically permutes the Casimirs.

Lemma 8.6. *The mutation sequences constructed above satisfy the following conditions:*

- *The first sequence of mutations permutes the Casimirs of Cases 2 and 3, leaving the Casimir of Case 1 unchanged. It also permutes the expressions for the minors defining the second conditions of Cases 2 and 3. Therefore, we conclude that the first sequence of mutations permutes Cases 2 and 3, leaving Case 1 unchanged.*
- *The second mutation sequence cyclically permutes Cases 1, 2, and 3.*

Remark 8.7. Since the transposition $(2,3)$ and 3-cycle $(1,2,3)$ generate the whole group S_3 of permutations of three elements, combining these sequences of mutations, one can obtain any permutation of Cases 1, 2, and 3.

Remark 8.8. As in the case $n = 5$, the coisotropic reduction for $n = 6$ leads to the cluster algebra containing all exponential shear coordinates as cluster variables and, therefore, all geodesic functions (symmetric or not) are universal Laurent polynomials of the square roots of these cluster variables.

Remark 8.9. In the paper [13], three sequences of mutations were constructed that act on the set of Casimirs. Let us introduce the following notation: $A = a_1a_2\dots a_6$, $B = b_1b_2\dots b_6$, $C = c_1c_2c_3$; $\hat{A} = ABC$, $\hat{B} = BC$, $\hat{C} = C$. The equalities $\hat{A} = \hat{B} = \hat{C} = 1$ correspond to the vanishing of anti-diagonal entries of matrix Ψ.

These sequences of mutations lead to the following rational transformations:

- $s_a\colon (A,B,C)\mapsto \big(A^{-1},AB,C\big)$;
- $s_b\colon (A,B,C)\mapsto \big(AB,B^{-1},BC\big)$;
- $s_c\colon (A,B,C)\mapsto \big(A,BC,C^{-1}\big)$.

Equivalently,

- $s_a\colon \big(\hat{A},\hat{B},\hat{C}\big)\mapsto \big(\hat{B},\hat{A},\hat{C}\big)$;
- $s_b\colon (A,B,C)\mapsto \big(\hat{A},\hat{C},\hat{B}\big)$;
- $s_c\colon (A,B,C)\mapsto \big(\hat{A}\hat{C}^{-1},\hat{B}\hat{C}^{-1},\hat{C}^{-1}\big)$.

Note that the subgroup generated by s_a, s_b acts as the permutation group S_3 on the triple of Casimirs $\hat{A}$, $\hat{B}$, $\hat{C}$. All three generators s_a, s_b, s_c satisfy the following relations: $s_a^2=s_b^2=s_c^2=1$, $(s_as_b)^3=1$, $(s_as_c)^2=1$, $(s_bs_c)^4=1$, i.e., s_a, s_b, s_c generate the Weyl group of type $B_3\simeq C_3$. It would be interesting to understand the connection between this Weyl group and the canonical braid group action on $\mathcal{A}_n$. In [13], the Weyl group acts on the moduli space of framed local systems on oriented surfaces by permutation of the eigenvalues and the change of flags of eigenvectors of monodromy operators. It might be interesting to find a similar geometric description of the Weyl group action on the symplectic groupoid. We are indebted to M. Berstein for this observation. Note, however, that mutation values $c_2=-1$ and $c_3=-1$ are not in the set of allowed values for mutations μ_{c_2} and μ_{c_3} so s_c is not allowed in the procedure of geometric reduction.

Remark 8.10. A. Shapiro and G. Schrader constructed an embedding of $U_q(\mathrm{GL}_n)$ into the quantum cluster algebra of framed local GL_n systems on a punctured torus with two marked points on the boundary. The latter has a natural Weyl group action, and elements of $U_q(\mathrm{GL}_n)$ are invariant with respect to this Weyl group action. L. Shen [17] proved that this embedding is, in fact, an isomorphism. Similarly, we assume that the algebra of regular functions on $\mathcal{A}_n$ is isomorphic to the subalgebra of elements of the cluster algebra invariant under the corresponding Weyl group action.

A Positivity condition for $n=5$

In this and the next appendices, we further investigate the coisotropic reduction to the geometric locus, taking into account the positivity of the cluster variables (exponentiated shear coordinates), which means that $h_i>0$ and $v_j>0$ in the case $n=5$. We solve this condition in terms of a_i, b_j with the coisotropic reduction condition imposed. Our main goal is to explore how the corresponding set of inequalities is transformed under the braid group action.

A.1 Inequalities for $\mathcal{A}_5$ cluster variables

A.1.1 The base system

Let $Q(x,y)=x^2y^2+2x^2y+x^2-2xy+2x+1$. The *base system* (A) that expresses the positivity condition for geometric cluster variables h_i, $i=1,\dots,4$, and v_j, $j=1,\dots,5$, reads

$$a_5=-\frac{1}{a_1a_2},\qquad a_1a_2a_3^2>0,\qquad a_1a_2a_3+a_1a_3+a_3>0,$$
$$a_5a_1a_4^2>0,\qquad a_5a_1a_4+a_5a_4+a_4>0,\qquad Q(a_1,a_2)>0,$$
$$b_1,b_2,b_3,b_4,b_5>0.$$

Note that, for $a_5a_1a_2=-1$, $Q(a_5,a_1)=\frac{1}{a_1^2a_2^2}Q(a_1,a_2)$, so $Q(a_5,a_1)>0$.

Equivalently, if

$$S := 1 + a_1(a_2 + 1), \qquad T := 1 + a_5(a_1 + 1),$$

then the two sign inequalities involving a_3 and a_4 are $a_3 S > 0$, $a_4 T > 0$.

From $a_5 = -1/(a_1 a_2)$ and $a_5 a_1 a_4^2 > 0$, one gets $a_2 < 0$. Then $a_1 a_2 a_3^2 > 0$ gives $a_1 < 0$. Write $a_1 = -u$, $a_2 = -r^2$, $u > 0$, $r > 0$. Then

$$a_5 = -\frac{1}{ur^2},$$

and the last quadratic inequality becomes

$$u^2\big(r^2 - 1\big)^2 - 2u\big(r^2 + 1\big) + 1 > 0.$$

Its roots are

$$\frac{1}{(r+1)^2}, \qquad \frac{1}{(r-1)^2}$$

when $r \neq 1$, and for $r = 1$ the same conclusion is obtained by taking the limit. Thus, the solution set of (A) has three sign components:

$$\text{(A.1)}\colon\ r > 1, \qquad u > \frac{1}{(r-1)^2}, \qquad a_3 > 0, \qquad a_4 > 0,$$

$$\text{(A.2)}\colon\ 0 < u < \frac{1}{(r+1)^2}, \qquad a_3 > 0, \qquad a_4 < 0,$$

$$\text{(A.3)}\colon\ 0 < r < 1, \qquad u > \frac{1}{(1-r)^2}, \qquad a_3 < 0, \qquad a_4 > 0.$$

For any choice of variables $(x_1, \dots, x_5, y_1, \dots, y_5)$, let $\mathcal{A}(x, y)$ denote the same system as (A), with a_i, b_i replaced by x_i, y_i:

$$x_5 = -\frac{1}{x_1 x_2}, \qquad x_1 x_2 x_3^2 > 0, \qquad x_3(1 + x_1(x_2 + 1)) > 0,$$
$$x_5 x_1 x_4^2 > 0, \qquad x_4(1 + x_5(x_1 + 1)) > 0, \qquad Q(x_1, x_2) > 0,$$
$$y_1, y_2, y_3, y_4, y_5 > 0.$$

A.1.2 Inverse formulas

Assume that the system (A) holds. Put

$$D := Q(a_1, a_2) = a_1^2 a_2^2 + 2a_1^2 a_2 + a_1^2 - 2a_1 a_2 + 2a_1 + 1.$$

The geometric cluster variables are then expressed via the $\mathcal{A}_5$ cluster variables (with the condition $a_1 a_2 a_5 = -1$ imposed):

$$h_1 = \frac{a_3}{2}\big(a_1 a_2 + a_1 + 1 - \sqrt{D}\big), \qquad h_4 = \frac{a_3}{2}\big(a_1 a_2 + a_1 + 1 + \sqrt{D}\big),$$
$$h_2 = \frac{a_4}{2a_1 a_2}\big(a_1 a_2 - a_1 - 1 - \sqrt{D}\big), \qquad h_3 = \frac{a_4}{2a_1 a_2}\big(a_1 a_2 - a_1 - 1 + \sqrt{D}\big).$$

A remarkable fact is that the above set of relations can be *inverted*, producing *rational* expressions for a_i in terms of the geometric cluster variables h_i, $i = 1, \dots, 4$:

$$a_1 = -\frac{h_2 h_3 (h_1 - h_4)^2}{h_1 h_4 (h_2 - h_3)^2}, \qquad a_2 = -\frac{(h_1 h_2 - h_3 h_4)^2}{h_2 h_3 (h_1 - h_4)^2},$$

$$a_3 = \frac{h_1h_4(h_2-h_3)}{h_1h_2-h_3h_4}, \qquad a_4 = \frac{h_1h_2-h_3h_4}{h_1-h_4},$$
$$a_5 = -\frac{h_1h_4(h_2-h_3)^2}{(h_1h_2-h_3h_4)^2}. \tag{A.1}$$

First, consider the Poisson transformation of geometric variables $h_j \to h_j^{-1}$ for $j = 1, \dots, 4$. The corresponding transformation for a_i,

$$a_i \to a_i, \qquad i = 1, 2, 5, \qquad a_3 \to (h_1h_4)^{-1}a_3, \qquad a_4 \to (h_2h_3)^{-1}a_4, \tag{A.2}$$

is a Poisson morphism.

All geometric cluster variables are independent and positive, $h_j > 0$. We then consider a subset $\mathcal{R}$ of h_j

$$\mathcal{R} := \mathbb{R}^4_+ \backslash \{h_1 = h_4 \vee h_2 = h_3 \vee h_1h_2 = h_3h_4\}$$

with singularities at $h_1 = h_4$, $h_2 = h_3$, and $h_1h_2 = h_3h_4$ removed. The domain $\mathcal{R}$ is then split into six nonintersecting domains in $\mathbb{R}^4_+$:

(I) $h_1 > h_4$ and $h_2 > h_3$ (then $h_1h_2 > h_3h_4$ and $a_3 > 0$ and $a_4 > 0$),
(II) $h_1 < h_4$ and $h_2 < h_3$ (then $h_1h_2 < h_3h_4$ and $a_3 > 0$ and $a_4 > 0$),
(III) $h_1 > h_4$ and $h_2 < h_3$ and $h_1h_2 < h_3h_4$ (then $a_3 > 0$ and $a_4 < 0$),
(IV) $h_1 < h_4$ and $h_2 > h_3$ and $h_1h_2 > h_3h_4$ (then $a_3 > 0$ and $a_4 < 0$),
(V) $h_1 > h_4$ and $h_2 < h_3$ and $h_1h_2 > h_3h_4$ (then $a_3 < 0$ and $a_4 > 0$),
(VI) $h_1 < h_4$ and $h_2 > h_3$ and $h_1h_2 < h_3h_4$ (then $a_3 < 0$ and $a_4 > 0$).

The sign components in the solution of system (A) therefore correspond to the respective sectors: (A.1) to (I)∪(II), (A.2) to (III)∪(IV), and (A.3) to (V)∪(VI), and the map $\{h_j\} \in \mathcal{R} \to \{a_i\}$ is therefore a double cover with variables in the dual sectors related by the transformation (A.2).[1]

Next we consider the action of braid-group transformations (maps) F, F_1, F_2 on system (A). These maps produce the corresponding systems (B), (C), (D). In all calculations below we always assume that all denominators do not vanish. The braid-group transformations on all quivers $\mathcal{A}_n$ are given by particular sequences of mutations derived in [4]. In the original $\mathcal{A}_5$-quiver in Figure 21, the four generators are $\Omega_i := \mu_{a_i}\mu_{a_{i+2}}\mu_{b_{i+1}}\mu_{a_{i+2}}\mu_{a_i}$ for $i = 1, \dots, 4$.

A.2 Case 1: The map F and system (B)

The map F corresponds to the braid-group transformation Ω_1. Define

$$X := a_1a_2a_3^2, \qquad S := 1 + a_1(a_2 + 1).$$

On (A), one has $X > 0$, $a_3S > 0$. Put

$$E := 1 + b_2(1 + a_3), \qquad C := 1 + b_2\big(1 + a_3(a_1 + 1)\big),$$
$$H := 1 + b_2(1 + X + a_3S), \qquad R := 1 + (1 + X + a_3S)b_2^2 + (2 + a_3S)b_2.$$

Then $H > 0$, $R > 0$. The map F can be equivalently written as

$$u_1 = \frac{a_1R}{C^2}, \qquad u_2 = \frac{a_2E^2}{R}, \qquad u_3 = \frac{a_3C}{HE},$$
$$u_4 = a_4E, \qquad u_5 = \frac{a_5C^2}{E^2}, \qquad v_1 = \frac{b_1H^2}{R},$$
$$v_2 = \frac{R}{a_1a_2a_3^2b_2}, \qquad v_3 = \frac{a_1a_2a_3^2b_3b_2^2}{R}, \qquad v_4 = b_4, \qquad v_5 = b_5.$$

The domain of this factored formula is $C \neq 0$, $E \neq 0$.

[1] We leave the problem of exploring boundary behavior of the reduction mappings to future work.

Derivation of system (B)

The first equality in (B) is just

$$u_5 = -\frac{1}{u_1 u_2},$$

because

$$u_1 u_2 = \frac{a_1 a_2 E^2}{C^2}.$$

Moreover,

$$u_1 u_2 u_3^2 = \frac{a_1 a_2 a_3^2}{H^2} > 0, \qquad u_3(1 + u_1(u_2 + 1)) = \frac{a_3 S}{H} > 0, \qquad u_5 u_1 u_4^2 = \big(a_5 a_1 a_4^2\big) R > 0.$$

For the fourth sign inequality, write $a_1 = -u$, $a_2 = -r^2$. Then

$$u_4(1 + u_5(u_1 + 1)) = -\frac{a_4 J}{a_1 a_2},$$

where

$$J = -\big(u\big(r^2 + 1\big) - 1\big) + b_2\big[-\big(u\big(r^2 + 1\big) - 1\big) + a_3\big(\big(1 - r^2\big)u^2 - \big(r^2 + 2\big)u + 1\big)\big].$$

In (A.1) and (A.3) one has $a_4 > 0$ and $J < 0$; in (A.2) one has $a_4 < 0$ and $J > 0$. Hence

$$u_4(1 + u_5(u_1 + 1)) > 0.$$

Finally,

$$Q(u_1, u_2) = \frac{E^2}{C^2} Q(a_1, a_2) > 0.$$

The inequalities $v_i > 0$ follow from $b_i > 0$, $H > 0$, $R > 0$, and $a_1 a_2 a_3^2 > 0$. Thus (A) implies (B) wherever F is defined.

Case correspondence for *F*

Since

$$\operatorname{sgn}(u_3) = \operatorname{sgn}(a_3)\operatorname{sgn}(C)\operatorname{sgn}(E), \qquad \operatorname{sgn}(u_4) = \operatorname{sgn}(a_4)\operatorname{sgn}(E),$$

the correspondence is

input component	extra condition	output component
(A.1)	$C > 0$	(B.1)
(A.1)	$C < 0$	(B.3)
(A.2)	always	(B.2)
(A.3)	$E > 0$	(B.3)
(A.3)	$E < 0$	(B.2)

where $C = 1 + b_2(1 + a_3(a_1 + 1))$, $E = 1 + b_2(1 + a_3)$. Thus

$$(\text{A.1}) \mapsto (\text{B.1}) \cup (\text{B.3}), \qquad (\text{A.2}) \mapsto (\text{B.2}), \qquad (\text{A.3}) \mapsto (\text{B.2}) \cup (\text{B.3}).$$

A.3 Case 2: The map F_1 and system (C)

The map F_1 corresponds to the braid-group transformation Ω_4. Keep

$$S := 1 + a_1(a_2 + 1), \qquad T := 1 + a_5(a_1 + 1).$$

Also put $Y := a_1 a_5 a_4^2$. On (A), $Y > 0$, $a_4 T > 0$. Define

$$E_1 := 1 + b_3(1 + a_4), \qquad G_1 := 1 + b_3(1 + a_4(1 + a_5)),$$
$$H_1 := 1 + b_3(1 + Y + a_4 T), \qquad R_1 := 1 + (1 + Y + a_4 T)b_3^2 + (2 + a_4 T)b_3.$$

Then $H_1 > 0$, $R_1 > 0$. Using $a_5 = -1/(a_1 a_2)$, the map F_1 becomes

$$u_1 = \frac{a_1 E_1^2}{R_1}, \qquad u_2 = \frac{a_2 G_1^2}{E_1^2}, \qquad u_3 = \frac{a_3 H_1}{G_1},$$
$$u_4 = \frac{a_4 G_1}{E_1 H_1}, \qquad u_5 = \frac{a_5 R_1}{G_1^2}, \qquad v_1 = b_1,$$
$$v_2 = b_2, \qquad v_3 = -\frac{a_2 R_1}{a_4^2 b_3}, \qquad v_4 = -\frac{a_4^2 b_4 b_3^2}{a_2 R_1}, \qquad v_5 = b_5 R_1.$$

The domain is $E_1 \neq 0$, $G_1 \neq 0$.

Derivation of system (C)

First,

$$u_5 = -\frac{1}{u_1 u_2}.$$

The basic sign inequalities factor as

$$u_1 u_2 u_3^2 = \frac{a_1 a_2 a_3^2 H_1^2}{R_1} > 0, \qquad u_5 u_1 u_4^2 = \frac{a_5 a_1 a_4^2}{H_1^2} > 0, \qquad Q(u_1, u_2) = \frac{E_1^2 G_1^2}{R_1^2} Q(a_1, a_2) > 0.$$

For the remaining two inequalities, define

$$L_1 := S + b_3(S(1 + a_4) - 2a_4), \qquad W := a_1 a_2 - a_1 - 1.$$

Then

$$u_3(1 + u_1(u_2 + 1)) = \frac{a_3 H_1 L_1}{R_1}, \qquad u_4(1 + u_5(u_1 + 1)) = \frac{a_4 W}{a_1 a_2 H_1}.$$

The factor L_1 has the same sign as S. Indeed, in (A.1) one has $S > 2$ and $a_4 > 0$, so

$$S(1 + a_4) - 2a_4 = S + a_4(S - 2) > 0.$$

In (A.2), one has $0 < S < 2$ and $a_4 < 0$, so the same expression is again positive. In (A.3), one has $S < 0$ and $a_4 > 0$, so it is negative. Hence $a_3 L_1 > 0$. Also $W = a_1 a_2 T$, and since $a_1 a_2 > 0$ and $a_4 T > 0$, one has $a_4 W > 0$. Therefore, the two remaining inequalities hold.

The inequalities $v_i > 0$ follow from $b_i > 0$, $a_2 < 0$, and $R_1 > 0$. Thus (A) implies (C) wherever F_1 is defined.

Case correspondence for F_1

Since

$$\operatorname{sgn}(u_3) = \operatorname{sgn}(a_3)\operatorname{sgn}(G_1), \qquad \operatorname{sgn}(u_4) = \operatorname{sgn}(a_4)\operatorname{sgn}(G_1)\operatorname{sgn}(E_1),$$

the correspondence is

input component	extra condition	output component
(A.1)	always	(C.1)
(A.2)	$E_1 > 0$	(C.2)
(A.2)	$E_1 < 0$	(C.1)
(A.3)	$G_1 > 0$	(C.3)
(A.3)	$G_1 < 0$	(C.2)

where $E_1 = 1 + b_3(1 + a_4)$, $G_1 = 1 + b_3(1 + a_4(1 + a_5))$. Thus

$$\text{(A.1)} \mapsto \text{(C.1)}, \qquad \text{(A.2)} \mapsto \text{(C.1)} \cup \text{(C.2)}, \qquad \text{(A.3)} \mapsto \text{(C.2)} \cup \text{(C.3)}.$$

A.4 Case 3: The map F_2 and system (D)

The map F_2 corresponds to the braid-group transformation Ω_2. Set $b = b_5$. Define

$$L_2 := 1 + b\ell_2, \qquad \ell_2 := 1 + a_3(1 + a_1(a_4 + 1)),$$
$$M_2 := 1 + bm_2, \qquad m_2 := 1 + a_1a_2(a_4 + 1)a_3^2 + (1 + (a_4 + 1)(a_2 + 1)a_1)a_3.$$

Next define

$$Y_2 := 1 + (a_4a_5(a_4 + 1)a_1 + 1 + a_4(a_5 + 1))a_2a_1a_3^2 + (1 + ((1 + a_4(a_5 + 1))a_2 + a_4 + 1)a_1)a_3,$$

and

$$N_2 := 1 + bY_2.$$

Finally, put

$$p_2 := 2 + (1 + ((1 + a_4(a_5 + 1))a_2 + a_4 + 1)a_1)a_3,$$
$$d_2 := 2 + (1 + a_4(a_5 + 1))a_1a_2a_3^2 + (2 + ((1 + a_4(a_5 + 1))a_2 + a_4 + 1)a_1)a_3,$$
$$\theta_2 := 2 + a_2(a_1a_5a_4 + 2 + a_4(a_5 + 1))a_1a_3^2 + (2 + ((2 + a_4(a_5 + 1))a_2 + a_4 + 2)a_1)a_3,$$

and

$$P_2 := 1 + Y_2b^2 + p_2b,$$
$$\Delta_2 := 1 + (1 + a_3)Y_2b^2 + d_2b,$$
$$\Theta_2 := 1 + \big(1 + a_1a_2a_3^2 + a_3S\big)Y_2b^2 + \theta_2b.$$

With these factors, the map F_2 becomes

$$u_1 = \frac{a_1P_2M_2^2}{L_2^2\Theta_2}, \qquad u_2 = \frac{a_2\Delta_2^2}{P_2M_2^2}, \qquad u_3 = \frac{a_3L_2}{\Delta_2},$$
$$u_4 = \frac{a_4\Delta_2}{M_2N_2}, \qquad u_5 = -\frac{L_2^2\Theta_2}{a_1a_2\Delta_2^2}, \qquad v_1 = -\frac{a_1a_3^2a_4^2b_1b^2}{P_2},$$
$$v_2 = b_2P_2, \qquad v_3 = \frac{b_3\Theta_2}{P_2}, \qquad v_4 = \frac{b_4N_2^2}{\Theta_2}, \qquad v_5 = -\frac{\Theta_2}{a_1a_3^2a_4^2b}.$$

The domain reads $L_2 \neq 0$, $M_2 \neq 0$, $\Delta_2 \neq 0$. The other potential denominators are automatically positive on (A), as explained below.

Sign facts for the factors

On (A), $Y_2 > 0$, $N_2 > 0$, $P_2 > 0$, $\Theta_2 > 0$. Furthermore,

input component	L_2	M_2	Δ_2
(A.1)	$\pm$	$+$	$+$
(A.2)	$+$	$\pm$	$+$
(A.3)	$+$	$+$	$\pm$

The signs not fixed by (A) are exactly the factors that distinguish the image component.

The verification is elementary after the substitution $a_1 = -u$, $a_2 = -r^2$. For example, in (A.1), one has

$$r > 1, \qquad u > \frac{1}{(r-1)^2},$$

so $u\big(r^2-1\big) > 1$. This makes the coefficients of M_2, Y_2, p_2, d_2, and θ_2 positive. Hence

$$M_2 > 0, \qquad P_2 > 0, \qquad \Delta_2 > 0, \qquad \Theta_2 > 0, \qquad N_2 > 0.$$

In (A.2), the inequality $u < 1/(r+1)^2$ gives the corresponding positivity of L_2, Y_2, p_2, d_2, θ_2. In (A.3), the inequalities $0 < r < 1$ and $u > 1/(1-r)^2$ imply $u\big(1-r^2\big) > 1$. This gives positivity of L_2, M_2, Y_2, p_2, θ_2, while Δ_2 may change sign.

Derivation of system (D)

The first equality in (D) is again

$$u_5 = -\frac{1}{u_1 u_2}.$$

The basic products reduce to

$$u_1 u_2 u_3^2 = \frac{a_1 a_2 a_3^2}{\Theta_2} > 0, \qquad u_5 u_1 u_4^2 = -\frac{P_2 a_4^2}{a_2 N_2^2} > 0,$$
$$Q(u_1, u_2) = \frac{M_2^2 \Delta_2^2}{L_2^2 \Theta_2^2} Q(a_1, a_2) > 0.$$

The positivity of the v_i's follows immediately from the displayed formula for F_2, because $a_1 < 0$, $P_2 > 0$, $\Theta_2 > 0$, $N_2 > 0$, $b_i > 0$.

It remains to record the two transformed mixed inequalities. Define $\Gamma_2 := S + b\gamma_2$, where

$$K_2 := \big((1 + a_4(a_5+1))a_2^2 + (2a_4+2)a_2 + a_4 + 1\big),$$
$$\gamma_2 = a_2(1 + ((1 + a_4(a_5+1))a_2 + a_4 + 1)a_1)a_1 a_3^2$$
$$\quad + \big(1 + K_2 a_1^2 + (2a_2 + a_4 + 2)a_1\big)a_3 + S.$$

Also define

$$\Lambda_2 := a_1^2 a_2 a_3 a_4 b + a_1^2 a_2 a_3 b + a_1^2 a_3 a_4 b + a_1^2 a_3 b - a_1 a_2 a_3 b - a_1 a_2 b - a_1 a_2$$
$$\quad + a_1 a_3 a_4 b + 2a_1 a_3 b + a_1 b + a_1 + a_3 b + b + 1.$$

A direct factorization gives

$$u_3(1 + u_1(u_2+1)) = \frac{a_3 \Gamma_2}{\Theta_2}, \qquad u_4(1 + u_5(u_1+1)) = -\frac{a_4 \Lambda_2}{a_1 a_2 N_2}.$$

Under (A), $a_3\Gamma_2 > 0$, $-a_4\Lambda_2 > 0$. Again this follows by substituting $a_1 = -u$, $a_2 = -r^2$ and using the three parameter ranges above. Therefore, the two remaining inequalities in (D) hold.

Thus (A) implies (D) wherever F_2 is defined.

Case correspondence for F_2

Since

$$\operatorname{sgn}(u_3) = \operatorname{sgn}(a_3)\operatorname{sgn}(L_2)\operatorname{sgn}(\Delta_2), \qquad \operatorname{sgn}(u_4) = \operatorname{sgn}(a_4)\operatorname{sgn}(M_2)\operatorname{sgn}(\Delta_2),$$

the correspondence is

input component	extra condition	output component
(A.1)	$L_2 > 0$	(D.1)
(A.1)	$L_2 < 0$	(D.3)
(A.2)	$M_2 > 0$	(D.2)
(A.2)	$M_2 < 0$	(D.1)
(A.3)	$\Delta_2 > 0$	(D.3)
(A.3)	$\Delta_2 < 0$	(D.2)

Thus

$$(\text{A.1}) \mapsto (\text{D.1}) \cup (\text{D.3}), \qquad (\text{A.2}) \mapsto (\text{D.1}) \cup (\text{D.2}), \qquad (\text{A.3}) \mapsto (\text{D.2}) \cup (\text{D.3}).$$

A.5 Summary of the three correspondences

We summarize our findings for $n = 5$ in the following table:

map	input component of (A)	output components
F	(A.1)	(B.1) ∪ (B.3)
F	(A.2)	(B.2)
F	(A.3)	(B.2) ∪ (B.3)
F_1	(A.1)	(C.1)
F_1	(A.2)	(C.1) ∪ (C.2)
F_1	(A.3)	(C.2) ∪ (C.3)
F_2	(A.1)	(D.1) ∪ (D.3)
F_2	(A.2)	(D.1) ∪ (D.2)
F_2	(A.3)	(D.2) ∪ (D.3)

All boundary cases where the splitting factor is zero are excluded from the corresponding rational map domain.

B Positivity condition for $n = 6$

We now turn to the case of $n = 6$; the analysis for even n seems to be easier since all transformations that occur are birational. To ensure positivity of all variables in the geometric quiver obtained by mutation and amalgamation, we first impose the coisotropic reduction condition

$$c_1c_2c_3 = 1, \qquad 1 + c_2 + c_2c_1 = 0, \qquad \text{or} \qquad c_1 = -1 - c_2^{-1}, \qquad c_3 = -(1 + c_2)^{-1}.$$

Then the condition that all cluster variables in the geometric quiver are positive can be split into the three sets of inequalities collected in the table below

	Case 1	Case 2	Case 3
c_2	< -1	$(-1,0)$	> 0
c_1	$(-1,0)$	> 0	< -1
c_3	> 0	< -1	$(-1,0)$
b_1	> 0	< 0	> 0
b_2	> 0	> 0	< 0
b_3	< 0	> 0	> 0
b_4	> 0	< 0	> 0
b_5	> 0	> 0	< 0
b_6	< 0	> 0	> 0

All variables a_i must be positive in all three cases.

We now perform the Dehn twist induced by a sequence of mutations $\mu_{b_1}\mu_{c_2}\mu_{b_3}\mu_{a_3}\mu_{b_3}\mu_{c_2}\mu_{b_1}$ in the $\mathcal{A}_6$ quiver. Retaining the labels of cluster variables, we have the following transformation law:

$$
\begin{aligned}
c_1' &= \frac{c_1c_2\varkappa}{c_2\varkappa+1}, & c_2' &= \frac{c_2\varkappa+1}{\varkappa-1}, & c_3' &= \frac{c_3(\varkappa-1)}{\varkappa},\\
b_1' &= \frac{\varkappa}{a_3}, & b_2' &= \frac{b_2a_3\eta}{(1+a_3)(\eta+1)}, & b_3' &= \frac{\eta+1}{c_2\varkappa},\\
b_4' &= \frac{b_4c_2\varkappa}{c_2\varkappa+1}, & b_5' &= b_5, & b_6' &= \frac{b_6(\varkappa-1)}{\varkappa},\\
a_1' &= \frac{a_1a_3}{1+a_3}, & a_2' &= a_2(1+a_3)(\eta+1), & a_3' &= \frac{1}{\eta},\\
a_4' &= \frac{a_4\eta}{\eta+1}, & a_5' &= a_5, & a_6' &= a_6,
\end{aligned}
$$

where

$$
\varkappa := 1 + b_1(1+a_3), \qquad \eta := b_3 + b_3c_2 + b_3c_2b_1 + b_3c_2b_1a_3. \tag{B.1}
$$

Observe, first, that

$$
c_1'c_2'c_3' = c_1c_2c_3 \qquad \text{and} \qquad 1 + c_2' + c_2'c_1' = \frac{\varkappa}{\varkappa-1}(1 + c_2 + c_2c_1),
$$

so the reduction conditions are preserved by the Dehn twist.

We next claim that $\eta > 0$ in all three cases. Indeed, when $c_2 > 0$, all variables in the corresponding expression in (B.1) are positive, so $\eta > 0$. When $c_2 < -1$, $b_3 < 0$ and $b_1 > 0$, so $b_1c_2b_3(1+a_3) > 0$ and $b_3(1+c_2) > 0$ and, therefore, $\eta > 0$; when finally $-1 < c_2 < 0$, $b_3 > 0$ and $b_1 < 0$ and then, again, $b_1c_2b_3(1+a_3) > 0$ and $b_3(1+c_2) > 0$, so $\eta > 0$. This immediately implies that all variables $a_i' > 0$ in all three cases. For the signs of b_i', we then have

$$
\begin{aligned}
&\operatorname{sgn} b_1' = \operatorname{sgn}\varkappa, && \operatorname{sgn} b_2' = \operatorname{sgn} b_2, && \operatorname{sgn} b_3' = \operatorname{sgn}(c_2\varkappa),\\
&\operatorname{sgn} b_4' = \operatorname{sgn}(b_4c_2\varkappa)\operatorname{sgn}(c_2\varkappa+1), && \operatorname{sgn} b_5' = \operatorname{sgn} b_5, && \operatorname{sgn} b_6' = \operatorname{sgn}(b_6(\varkappa-1)\varkappa).
\end{aligned}
$$

B.1 Case 3

The simplest case is Case 3 in which $c_2 > 0$. Then $b_1 > 0$ and $\varkappa > 1$, so $c_2' = \frac{c_2\varkappa+1}{\varkappa-1} > 0$, b_2' and b_5' are negative, all other b_i' are positive, and we obtain again Case 3 for the transformed variables.

B.2 Case 1

Let $c_2 < -1$. Then $b_1 > 0$, $\varkappa > 1$ and $c_2' + 1 = (c_2 + 1)\frac{\varkappa}{\varkappa - 1} < 0$, so $c_2' < -1$. In this case, $c_2\varkappa + 1 < 0$, and it is easy to see that all b_i' are positive except b_3' and b_6', so we again obtain Case 1.

B.3 Case 2

The only nontrivial situation occurs in Case 2: $-1 < c_2 < 0$. In this case, $b_1 < 0$ and $\varkappa < 1$. We consider separately two subcases:

B.3.1 Subcase $0 < \varkappa < 1$

In this case, $c_2\varkappa + 1 > 0$, and we have that

$$c_2' + 1 = (c_2 + 1)\frac{\varkappa}{\varkappa - 1} < 0.$$

The variables b_2', b_5', b_1', and b_4' are positive, whereas b_3' and b_6' are negative. Thus we obtain Case 1.

B.3.2 Subcase $\varkappa < 0$

In this case, again, $c_2\varkappa + 1 > 0$, and $c_2' + 1 > 0$ but $c_2' < 0$. We also have that $b_1' < 0$ and $b_4' < 0$ while all other b_i' are positive, so we obtain Case 2.

We summarize the results of this section in the following table:

input	Case 1	Case 2, $\varkappa > 0$	Case 2, $\varkappa < 0$	Case 3
output	Case 1	Case 1	Case 2	Case 3

Remark B.1. Note that unlike the case $n = 5$, in the $n = 6$ case, as well as in all higher-rank cases, we cannot express $\mathcal{A}_n$ cluster variables in terms of the geometric cluster variables, and each of the three cases covers the entire Teichmüller space parameterized by shear coordinates. This is because the constraint $1 + c_2^{-1} + c_2^{-1}c_3^{-1} = 0$ with $c_1c_2c_3 = 1$ is Lagrangian: all composite geometric cluster variables Poisson commute with this constraint on the constraint surface. The product of the c_i is a Casimir of the full algebra and therefore Poisson-commutes with all combinations of variables; by contrast, the second condition results in additional dimensional reduction.

C Commutativity of reduction mapping and braid-group action

Let $B_{i,i+1}$ and $\widetilde{B}_{i,i+1}$, $i = 1, \ldots, n-1$, denote the respective (invertible) braid-group transformations of cluster variables in the $\mathcal{A}_n$-quiver and in the geometric quivers $\mathcal{G}_n$. (The sequences of mutations Ω_i are $B_{i,i+1}$ in the case $n = 5$.) We let $\mathcal{R}$ denote the reduction mapping from $\mathcal{A}_n$ to $\mathcal{G}_n$ (this mapping is not invertible for a general n). We checked by explicit calculations using AI-assisted symbolic computations that the diagram

$$\begin{array}{ccc} \mathcal{A}_n & \xrightarrow{\mathcal{R}} & \mathcal{G}_n \\ {\scriptstyle B_{i,i+1}}\downarrow & & \downarrow{\scriptstyle \widetilde{B}_{i,i+1}} \\ \mathcal{A}_n & \xrightarrow{\mathcal{R}} & \mathcal{G}_n \end{array}$$

is commutative for $n = 5, 6$ in all cases considered above.

Acknowledgements

The project started under the umbrella of the "Discovering America" program at Michigan State University, hosting one-semester joint research teams of visiting students from China and groups of US students. The authors are grateful to the Math Department of Michigan State University for its hospitality, support, and inspiring research atmosphere, which enabled us to continue the research that led to this publication. Special thanks are due to Linhui Shen, Francis Bonahon, Alexander Shapiro, and Michael Berstein for the valuable discussions. M.S. was partially supported by the NSF research grant DMS #2100791.

The computations presented in Appendices A and C were initially carried out with the assistance of ChatGPT (GPT-5.5). All results were subsequently independently verified by the authors, who take full responsibility for their correctness.

We are especially grateful to the anonymous referees for their careful reading and valuable suggestions, which have significantly improved the quality of this paper.

References

[1] Boalch P.P., Stokes matrices, Poisson Lie groups and Frobenius manifolds, *Invent. Math.* **146** (2001), 479–506, arXiv:math/0011062.

[2] Bondal A.I., A symplectic groupoid of triangular bilinear forms and the braid group, *Izv. Math.* **68** (2004), 659–708.

[3] Chekhov L.O., Fock V.V., Observables in 3D gravity and geodesic algebras, *Czechoslovak J. Phys.* **50** (2000), 1201–1208.

[4] Chekhov L.O., Shapiro M., Log-canonical coordinates for symplectic groupoid and cluster algebras, *Int. Math. Res. Not.* **2023** (2023), 9565–9652, arXiv:2003.07499.

[5] Chekhov L.O., Shapiro M.Z., Shibo H., Roots of the characteristic equation for the symplectic groupoid, *Russian Math. Surveys* **77** (2022), 552–554, arXiv:2101.10323.

[6] Fock V.V., Description of moduli space of projective structures via fat graphs, arXiv:hep-th/9312193.

[7] Fock V.V., Goncharov A.B., Moduli spaces of local systems and higher Teichmüller theory, *Publ. Math. Inst. Hautes Études Sci.* **103** (2006), 1–211, arXiv:math/0311149.

[8] Fomin S., Shapiro M., Thurston D., Cluster algebras and triangulated surfaces. Part I: Cluster complexes, *Acta Math.* **201** (2008), 83–146, arXiv:math/0608367.

[9] Fomin S., Zelevinsky A., Cluster algebras I: Foundations, *J. Amer. Math. Soc.* **15** (2002), 497–529, arXiv:math/0104151.

[10] Gekhtman M., Shapiro M., Vainshtein A., Cluster algebras and Poisson geometry, *Mosc. Math. J.* **3** (2003), 899–934, arXiv:math/0208033.

[11] Gekhtman M., Shapiro M., Vainshtein A., Cluster algebras and Weil–Petersson forms, *Duke Math. J.* **127** (2005), 291–311, arXiv:math/0309138.

[12] Gekhtman M., Shapiro M., Vainshtein A., Cluster algebras and Poisson geometry, *Math. Surveys Monogr.*, Vol. 167, American Mathematical Society, Providence, RI, 2010.

[13] Goncharov A., Shen L., Donaldson–Thomas transformations of moduli spaces of G-local systems, *Adv. Math.* **327** (2018), 225–348, arXiv:1602.06479.

[14] Nelson J.E., Regge T., Homotopy groups and $(2+1)$-dimensional quantum gravity, *Nuclear Phys. B* **328** (1989), 190–202.

[15] Nelson J.E., Regge T., Zertuche F., Homotopy groups and $(2+1)$-dimensional quantum de Sitter gravity, *Nuclear Phys. B* **339** (1990), 516–532.

[16] Postnikov A., Total positivity, Grassmannians, and networks, arXiv:math/0609764.

[17] Shen L., Cluster nature of quantum groups, arXiv:2209.06258.

[18] Weinstein A., Symplectic groupoids and Poisson manifolds, *Bull. Amer. Math. Soc. (N.S.)* **16** (1987), 101–104.